University of Nottingham
UK | CHINA | MALAYSIA

AN INVESTIGATION INTO THE RELATIONSHIP BETWEEN SYNTHETIC APERTURE RADAR (SAR) DATA AND BEACH SEDIMENT GRAIN SIZE

Sophie Jean **Mann**
Student ID: 14329469

Nottingham Geospatial Institute, University of Nottingham, UK

Dissertation submitted to The University of Nottingham in partial fulfilment of the degree of Master of Research in Geospatial Systems

August 2022

ABSTRACT

Sediment grain size on beaches has been established as a crucial parameter to determine shoreline changes and provide coastal protection. However, traditional surveying techniques are time-consuming, with records becoming outdated quickly. The use of Synthetic Aperture Radar (SAR) data for this application will enable quick surveying of beaches and is particularly useful due to the ability to collect data irrespective of weather-conditions. This study aims to evaluate if there is a relationship between sediment grain size on beaches and the backscatter from satellite SAR data. As part of this investigation, a fieldwork methodology has been constructed and carried out to obtain ground-truth data for beach sediment grain size and elevation. Results show a strong positive correlation between backscatter from C-band Sentinel-1 data and median sediment grain size on beaches. However, only a moderate correlation was found between backscatter from S-band NovaSAR data and median sediment grain size. These results are mainly attributed to the size of the sediment analysed in this study, compared to the SAR wavelength, along with increasing surface roughness as sediment size increases.

Declaration: "I hereby certify that this work is my own, except where otherwise acknowledged, and that it has not been submitted previously for a degree at this, or any other university."

ACKNOWLEDGEMENTS

CONTENTS

LIST OF FIGURES

LIST OF TABLES

LIST OF ABBREVIATIONS

ALOS - Advanced Land Observing Satellite

cm – centimetres

dB – Decibel units

ERS - European Remote Sensing satellite

ESA – European Space Agency

GIS – Geographic Information System

GNSS - Global Navigation Satellite System

HH – Horizontal-Horizontal Polarisation

HV – Horizontal-Vertical Polarisation

IPR – Image Processing Research

JERS - Japanese Earth Resources Satellite

m – metres

mm – millimetres

NASA JPL - National Aeronautics and Space Administration Jet Propulsion Laboratory

RTK – Real Time Kinematic

SAR – Synthetic Aperture Radar

SMPs – Shoreline Management Plans

UKHO – UK Hydrographic Office

VH – Vertical-Horizontal Polarisation

VV – Vertical-Vertical Polarisation

$\sigma°$ - Sigma Naught (Sigma0)

1. INTRODUCTION

1.1 Monitoring of Beach Sediment Grain Size

Sediment grain size is a vital parameter which determines both beach morphology and shoreline changes (Cabezas-Rabadán et al., 2021). The monitoring of these sediments is becoming increasingly important to determine sediment transportation and coastal morphodynamics (Bio et al., 2015). Therefore, sediment grain size is a pivotal element to measure to understand coastal dynamics and in turn, improve beach management and protection.

Traditional surveying techniques to determine coastal sediment size are very time consuming and costly, especially when surveying large areas (Chardon et al., 2020; Cabezas-Rabadán et al., 2021). These methods also become even more challenging due to the dynamic nature of these environments, meaning that surveys will need to be carried out regularly.

The study of sediment grain size in coastal areas also has additional benefits, including increased geological knowledge, better information for navigation, and greater informed coastal management, for example, deciding where is best to place sea defences along a coastline (Deroin, 2020).

As a result of this, the study into the use of remotely sensed methods for monitoring coastal sediments have become prominent in recent years.

1.2 Coastal Sediment Transportation

Waves, tides, and currents are the dominant forces which influence both; the sediment deposited on beaches and the area on the beach in which it is deposited (Davis and Fitzgerald, 2004). The process of longshore drift (Figure 1) determines the direction of transport along the coastline. This is caused by a longshore current (littoral current), produced by wave refraction as a result of the prevailing wind direction, which in turn, causes the transportation of sediment (Davis and Fitzgerald, 2004).

This figure cannot be reproduced due to copyright.

Figure 1: A simplified diagram showing longshore drift. The prevailing wind direction controls the angle the waves approach the beach, and the longshore current. This controls the path of transportation and the subsequent net movement of sediment. Source: Uncles et al., (2020).

1.3 Coastal Erosion

Coastal environments are highly dynamic environments. Beaches offer plentiful benefits. They provide coastal protection, creating a natural barrier by absorbing wave energy before it reaches the cliffs, provide a habitat for multiple species, and provide recreational activities for coastal societies (Cabezas-Rabadán et al., 2021).

However, coastal erosion poses a significant risk to much of the UK's coastline and coastal communities. Masselink et al., (2020) found that almost 1/5th of the UK's coastline is suffering from some form of erosion. The impacts of this erosion are vast, having a huge economic and societal impact. As coastal areas are home to a large population, with over 5.3 million people living in coastal areas in England and Wales as of October 2020 (ONS, 2020), coastal erosion can devastate coastal communities through loss of properties and livelihoods.

Shoreline Management Plans (SMPs) are documents which detail how coastal erosion and flood risks should be managed in each area. These are based upon the sediment cell principle (Williams et al., 2018). This principle is described by Zikra and Suntoyo (2017) as individual coastal areas in which the coastal landforms and geomorphology are likely to be connected due to sediment exchange processes and transportation. Therefore, this research is relevant to the determination of sediment cells and can help with shoreline management. This is because knowledge of sediment grain size can be an indicator of sediment transportation patterns, due to the littoral erosion processes discussed above.

Anthropogenic climate change has also made these coastal environments increasingly vulnerable. The susceptibility of coasts to coastal erosion is increasing due to rising sea levels and an increase in the frequency and severity of storms (Vitousek et al., 2017). These extreme storms events can cause enhanced erosion on cliffs and beaches (Harley et al., 2022). As these negative impacts from climate change are predicted to worsen, efficient monitoring of coastal areas has never been more imperative.

1.4 Synthetic Aperture Radar (SAR)

The origins of SAR date back to 1951, where it was invented by a mathematician named Carl A. Wiley (Wiley, 1985). The first SAR satellite, Seasat, was launched by NASA JPL in 1974, providing, for the first time, SAR data for use in earth observation studies (Born et al., 1979). Born et al., (1979) describe how the satellite originally was intended for ocean applications and was able to capture SAR data of 95 % of the earth's oceans every 36 hours. Seasat failed after less than 4 months in orbit, in October 1974, due to an electrical fault, but during its short lifespan, managed to collect a vast amount of oceanographic data, on winds, waves tides and currents (Born et al., 1979).

Since the launch of Seasat, there have been multiple SAR satellites launched into orbit. Some of the most notable SAR satellites being RADARSAT 1 and 2, JERS-1, ERS 1 and 2, and Sentinel-1. The launch of these satellites has enabled huge advances in the use of SAR data in earth observation, with popular applications of SAR being in the fields of forestry and agriculture, amongst others. As of 2021, there are nearly 50 SAR satellites currently operating, more than double the amount operating in 2018, attributed to a rise in commercial interest (Rosen [online], 2021).

1.5 Principles of SAR

One of the basic principles of SAR which is highly relevant to this study is that, in general, radar waves interact with the objects which have the same or larger spatial magnitude as the wavelength of the radar signal, which differs with satellites of different radar bands (Rosenqvist et al., 2018). If the object is considerably smaller than the wavelength, they are not picked up by the radar signal, as they become transparent, and therefore, although they may cause some attenuation of the signal, these objects will have a significantly less effect on the backscatter (Rosenqvist et al., 2018).

Polarimetry is also an important aspect in SAR. In simple terms, the SAR polarimetry describes the direction in which the electromagnetic wave is pointing to and hence, where radar signal is emitted from (Woodhouse, 2006). Where the polarimetry is uniform, e.g., VV (vertical-vertical polarisation), this is known as co-polarisation, whereas a differing polarimetry, e.g., VH (vertical-horizontal polarisation), is known as cross-polarisation.

There are multiple types of scattering, the type of which will happen depends on how the radar signal interacts with the target. The exact scattering mechanisms from radar are not fully understood, however, there are some widely accepted scattering theories. The main types of scattering with potential to relate to this study are outlined and displayed visually below (Figure 2).

This figure cannot be reproduced due to copyright.

Figure 2: Diagrams showing SAR scattering mechanisms. a. Direct scattering, b. Forward scattering on a smooth surface, c. Diffuse scattering on a rough surface, d. Double-bounce diffuse-type scattering. Source: Rosenqvist et al., (2018).

Direct backscattering is when the radar signal is directly reflected back to the sensor and usually occurs when the surface is orientated perpendicular to the direction of the radar satellite and causes the part of the image where this scattering occurs to look bright and have a strong co-polarisation reflection in HH or VV polarisations (Figure 2a) (Rosenqvist et al., 2018). Forward scattering occurs when the surface reflects the signal away from the radar sensor, resulting in little or no backscattering towards the sensor (Figure 2b)

(Rosenqvist et al., 2018). This usually occurs on smooth surfaces, for example, calm water. Figure 2c shows diffuse scattering, where in the radar signal is scattered in multiple directions from a rough surface, for instance, where choppy waves are present in water (Rosenqvist et al., 2018). According to Woodhouse (2006), a greater co-polarisation return is associated with smoother surfaces, compared to a greater cross-polarisation, which is associated with rougher surfaces.

Double-bounce scattering has two main types of scattering: diffuse and specular type. Diffuse-type double bounce scattering is relevant to this study as it occurs when an object, e.g., a cliff, lies perpendicular to a rough surface, which acts as a corner reflector and causes a double-bounce scattering, as well as scattering within the rough surface, which results in a greater return signal and only occurs with co-polarisation (Figure 2d) (Rosenqvist et al., 2018).

1.6 SAR Backscatter

Radar backscatter is defined as the amount of radar signal that is redirected back to the sensor by the target (ESA [online], 2022a). The backscattering coefficient is expressed in terms of σ^0 (Sigma0) and is usually expressed in decibel units (dB) (Rosenqvist et al., 2018). When interpreting a SAR image, the general rule is the rougher the surface, which is being imaged, a higher backscatter intensity, in both cross- and co-polarisation, will be observed and the brighter the image will look (Liew [online], 2001; Alaska Satellite Facility, 2022). This is because a smooth surface will cause specular reflection, meaning that the radar signal reflects away from the target, resulting in limited radar return, whereas a rough surface causes various types of scattering, resulting in a greater amount of the radar signal returning to the target (IPR [online], 2022) (Figure 3). The backscattering coefficient represents a normalised radar cross-section and is measured in decibel units (dB), which range from values of +5 dB for rough surfaces which appear very bright in a radar image, such as mountains and trees, to -40 dB for smoother surfaces, which appear very dim in a radar image, such as bodies of water (Liew [online], 2001; IPR [online], 2022).
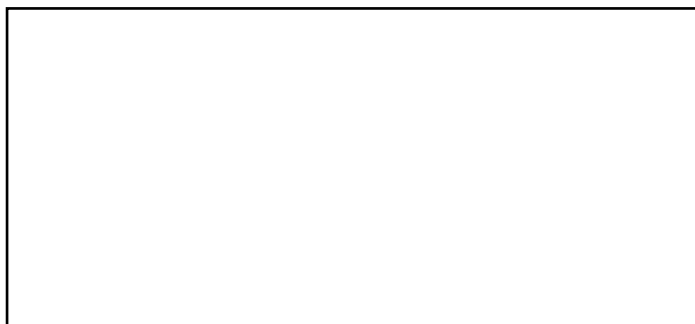
This figure cannot be reproduced due to copyright.

Figure 3: A diagram showing radar scattering on (a) smooth surfaces, which results in no or limited radar return and (b) rough surfaces, which results in a greater amount of radar return. Source: IPR (Image Processing Research, 2022).

1.7 S-band SAR

The use of S-band SAR has been limited thus far. This is one of the reasonings behind the development and deployment of NovaSAR-1, a S-band SAR satellite, launched in

September 2018 by SSTL and Airbus Defence and Space (Whittaker et al., 2021). Previously, the last notable S-band SAR mission was the Russian Almaz-1 satellite which was decommissioned in 1992 (Natale et al., 2011).

Due to S-band SAR having a wavelength that is relatively close to C-band SAR, the applications are broadly thought to be most similar to those of C-band SAR (Natale et al., 2011). The NovaSAR-1 satellite, in which data is used in this study, operates at a frequency of 2-4 GHz and has a wavelength of 7.5-15 cm (Herndon et al., [online], 2019).

The NovaSAR mission was designed to have a wide range of applications, including maritime surveillance, disaster monitoring and studies of forests and vegetation (Bird et al., 2013). CSIRO (2021) also outline coastal habitat and geological mapping as one of the key applications in which they hope to utilise NovaSAR data for, which is very relevant to this study. Whittaker et al., (2021) collated the applications and mission achievements of NovaSAR as of 2021 and presented that the images over land can clearly identify urban infrastructure and can differentiate types of vegetation. They also discuss how there is also promising ocean applications, including studies into wave structure and sea ice. Despite the stated applications of this satellite, there has yet to be any research publications which detail the use of S-band to determine beach sediment grain size or specifically focusing on analysing the backscatter from NovaSAR data in coastal areas.

This satellite is still a novel satellite and has 3 more years, as of 2022, in-orbit lifespan for data collection, so it is hopefully that research using NovaSAR data will increase as the satellite becomes more renowned.

1.8 C-band SAR

C-band SAR data has been widely used in multiple studies. This can be attributed to the high availability of C-band SAR data, due to the availability of data from ESA's Sentinel-1 satellites, resulting in this data being used in multiple studies for multiple applications (Potin et al., 2016). C-band SAR has an associated frequency of 4-8 GHz and a wavelength of 3.8-7.5 cm (Herndon et al., [online], 2019). The Sentinel-1 satellite constellation, Sentinel-1A and Sentinel-1B, have a revisit period of up to 12 days, and operates in four image modes, each providing contrasting resolution and coverage (Geudtner et al., 2014). Since December 2021, Sentinel-1B suffered a major failure, and as a result, ceased data collection (ESA [online], 2022b). As a result of this, data collection has been solely reliant on Sentinel-1A.

1.8 Aims and Objectives

The aims and objectives of this research project are outlined below:

Aim: The aim of this study is to investigate the relationship between SAR backscatter and the sediment grain size on beaches.

Objectives:

1. To determine sediment grain size distribution on a range of beaches by constructing and carrying out a fieldwork methodology to collect ground-truth data for beach composition.
2. Evaluate if there is a correlation between backscatter from SAR imagery and sediment size.
3. Evaluate whether sediment size can be determined from the profile of a beach, specifically looking at the beach elevation and gradient.

Research Question

Therefore, derived from these objectives, the main research question is as follows:

What is the relationship between sediment grain size and SAR backscatter?

Hypothesis

Although there have been limited studies in this area, based on Wu et al., (2019)'s findings, and understanding the mechanisms of SAR backscatter, it can be hypothesised that a greater backscatter coefficient is indicative of a larger sediment size.

2. LITERATURE REVIEW

2.1 SAR and Sediment Grain Size

The use of SAR data to determine the grain size of beach sediment is an obvious choice as it has the capabilities to collect high-resolution data independent of weather (i.e., it is not affected by clouds or adverse weather conditions) and is able to collect data in the day or night (Enomoto et al., 2018). These factors are especially useful for this application as it allows data to be collected frequently in any conditions, allowing for regular beach monitoring, especially after or during a storm to determine how said storm has influenced the sediment.

Therefore, it is somewhat surprising to note, that despite this useful application, there have been limited studies into the relationship between coastal sediments and SAR backscatter to date. As part of a study on using SAR data for coastline detection, Wu et al., (2019) investigated the relationship that various sized coastal sediment has on SAR backscatter for several beaches across Japan. They used data from ALOS-2, which is equipped with PLASAR-2, a L-band SAR sensor, with a wavelength of approximately 24 cm. A strong correlation was found between the mean backscatter and median diameter of the beach materials (Figure 4) (Wu et al., 2019).

Figure 4: A graph to show the mean beach backscatter coefficient plotted against the median diameter of the beach material (D_{50}) for several beaches across Japan. Source: Wu et al., (2019).

It was found that the *Nami-ita, Shiraho* and *Fuji* coasts, which consisted of coarse sediments; coarse gravel, and coral gravels, had a significantly greater mean
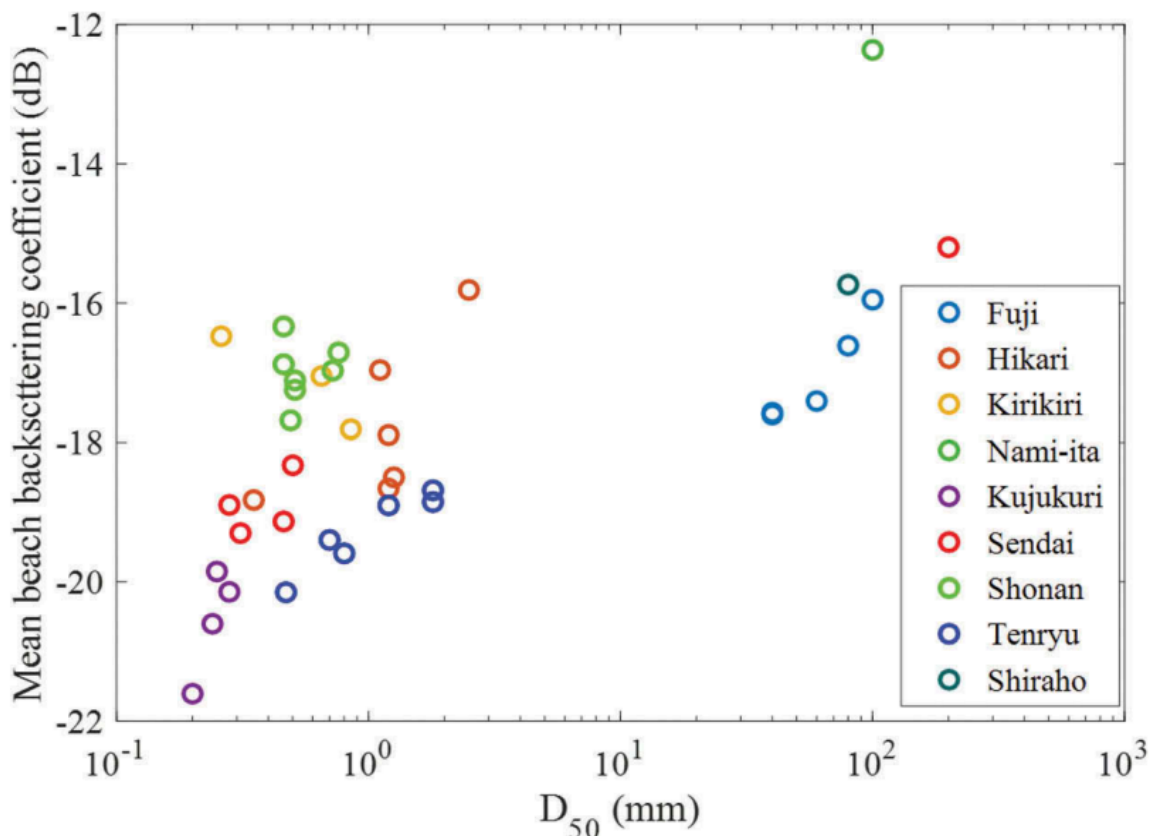
backscattering coefficient, compared to those beaches which consist of smaller gravel and sand, which had a lower mean beach backscattering coefficient (Wu et al., 2019).

However, although the study found a strong correlation between the two variables, there were some outliers to the overall trend. For example, beaches on the *Sendai* coast generally consist of fine, sandy materials and thus, had a lower backscatter coefficient. However, one beach on this coast had a higher backscattering coefficient of -15.2 dB due to the presence of larger rocks on the beach (Wu et al., 2019). This demonstrates that whilst using the median sediment grain size on the beach is preferable, as it is more resistant to outliers in sediment grain size, it can misrepresent the actual beach sediment structure. Furthermore, the study found that although both the *Nami-ita* and *Fuji* coast have a similar median grain size, the *Nami-ita* coast had a much higher mean dB, it was suggested that this could be attributed to the cusp profile of the *Nami-ita* coast, which, in turn, will increase the surface roughness of the beach (Wu et al., 2019). Such evidence demonstrates that in some instances, multiple factors, other than just grain size, can be attributed to the differences observed in mean backscatter.

Van der Wal et al., (2005) used ERS C-band SAR imagery to study characteristics of intertidal flats in the Netherlands. Their study found similar results to Wu et al.'s (2019) study; a significant positive correlation between the sediment grain size of the intertidal flats and SAR backscatter (van der Wal et al., 2005). They attributed this positive correlation to the fact that surface roughness increased as median grain size and decreased when an area had a high mud content, thus a lower median grain size. In this study, they were able to rule out surface moisture content as a factor influencing the SAR backscatter, due to the surface moisture being high across all the sites they investigated, and so this meant that they could attribute the variations seen in the backscatter to other factors; one of these factors being sediment grain size on the flats (van der Wal et al., 2005). However, this study only looked at sediment size with a median grain size of up to 1 mm, as sediments larger than this were discarded as part of the study. This median grain size is much smaller than some of the grain sizes used in this study and in the study by Wu et al., (2019).

A study by Stark et al., (2018) explored the potential of using SAR data to carry out a geotechnical analysis of beach sediments. The study used some preliminary data from X-band SAR. They identified sediment grain size as one of the key soil parameters, alongside soil moisture content and beach slope, which determines surface attributes and structural properties and thus, has an influence on SAR backscatter (Stark et al., 2018). An assumption was made that the beach slope is constant, and the beach surface sediments are loosely deposited, therefore, leaving the grain size distribution the main factor in which controls the surface roughness, with the surface moisture content being a distinctive variable (Stark et al., 2018). However, this is not always the case, as beach slope is not always constant along a single beach. Regardless of this, the study showed promising results, including findings that a strong backscatter can be found in areas which have vegetated sand dunes and a lower backscatter on dry sand areas (Stark et al., 2018). However, this study relies heavily on analysing the changes on surface moisture content of the beach, which may not be present in beaches with coarser sediment size, to characterise the sediment. Subsequently, the study is more focused on determining the sediment properties, i.e., sediment strength, friction angles and moisture content (Stark et al., 2018) than ascertaining the median grain size on the beach.

2.2 External Factors Influencing SAR Backscatter

SAR backscatter can be affected by many other external factors, other than just the grain size of the beach materials, in coastal areas. Deroin (2020) studied the potential of Sentinel-1 for mapping intertidal flats and found that the dielectric properties of the surface (moisture and salinity) influence the radar backscatter. Therefore, gently sloped tidal flats have minimal scattering and a lower backscatter due to a high amount of surface moisture (Deroin, 2020). This is important when considering the intertidal areas of the beach, especially on sandy beaches. Conversely, whilst Wu et al., (2019) conceded that tidal level will alter the moisture content of the beach, after comparison of multiple SAR images at different tidal levels, they found no significant relationship between tidal level and backscattering coefficient in their study. A study by Brakenhoff et al., (2019) states that if the beach elevation is greater than 0.5 m above the high tide level, then the water table will be too deep to influence the soil moisture. Therefore, the knowledge of tide data at the time in which the SAR imagery was acquired is highly important, in addition to knowing the elevation of the beach. It could be proposed that the reason why Wu et al., (2019) did not find that tidal level influenced backscatter, in contrast to Deroin (2020) who did find a correlation, is because the beaches studied by Wu et al., (2019) could have had a higher elevation above tidal level, and therefore moisture would not have had an impact on these beaches, in contrast to Deroin's (2020) study, whereby the low elevation means that moisture would have had a big impact on the intertidal flats.

Surface roughness (i.e. surface texture) was another factor Deroin (2020) outlined as having a strong influence on radar backscatter. Van der Wal et al., (2005) also attributed this as one of the main causes of the difference observed in backscatter on intertidal flats. Sano et al., (1999) found a relatively strong correlation between the backscatter for ERS-1 SAR and surface roughness, however, this study was not based on coastal areas and did not yield a definitive result that it is possible to predict surface roughness from SAR data, due to the influence of moisture.

Stark et al., (2018) found that vegetated dunes had a high backscattering coefficient, due to the presence of the vegetation. Vegetated sand dunes were not present in any of the areas where data was collected in this study. However, consideration will need to be given to this theory if SAR data on beaches with vegetated sand dune present are analysed in further research.

2.3 Fieldwork Methodology

Multiple previous studies have carried out fieldwork investigations alongside the use of remotely sensed data to classify sediment (Kim et al., 2019).

The fieldwork methodology which will be used in this study is based on that of van der Wal et al., (2005), who carried out fieldwork to support the use of SAR imagery to characterise surface roughness and sediment texture on intertidal flats. Conversely, the same methodology was then repeated two years later in another study by van der Wal and Herman (2007), establishing it as a robust fieldwork methodology, which has been used in two well-cited research studies; both of which use SAR data for sediment characterisation. The fieldwork method used in these studies collected 20 cm³ of sediment from the upper 3 cm of sediment, taken 30-60 m apart, during low tide (van der Wal et al., 2005; van der Wal and Herman, 2007). However, they collected samples over the course of 9 years (1995-2004), which was not viable for this current study, given the time constraints. The distance between sample collection was also increased for this study, due to the need to get an overview of a whole beach within a limited

designated time-period for fieldwork. The exact methodology to collect the data used to determine the median sediment grain size in the study by Wu et al., (2019) is unknown.

Van der Wal et al., (2005) and van der Wal and Herman's (2007) methodology was predominantly used to collect sand. So, as part of pebble selection and measurement, methods to measure the median sediment size were deliberated upon. One of these methods is the Wolman's (1954) pebble count. This is where pebbles are selected and measured at random, often along a certain specified distance. Many previous studies have used this method, including a recent study by Lees et al., (2022), which successfully used the method to measure superficial clasts in gravel beaches. Strom et al., (2010) states that this method is useful to measure the grain size of the surface layer of pebbles, which is what is required in this study. They also state that another advantage of this method is that it requires little field equipment, which is especially advantageous when collecting pebbles in relatively remote locations, such as beaches. There are, however, disadvantages of using this methodology as both Strom et al., (2010) and Harvey et al., (2022) have reported bias. Specifically, both papers identified that sediment grain size was overestimated, meaning that sediments were recorded as being coarser than the actual beach median.

Another methodology to measure pebble size was deliberated upon to use in this study. Outlined by Harvey et al., (2022), this method is less field intensive, using photo analysis to manually measure the pebble size. Although this methodology is advantageous as it can be used to determine sediment size in any area where the imagery, usually collected by UAVs, is available, if the spatial resolution is not higher than the sediment size present then this method will either be unable to be used or there will be a strong bias towards the sampling of the bigger sediments (Harvey et al., 2022).

Therefore, given that the use of UAVs was unavailable, the small size of pebbles in some locations, relatively remote location of some of the field sites, and the short time scale of this ambitious project, the Wolman's (1954) pebble count was considered sufficient.

To analyse the results in this study, scatter graphs and regression models were chosen as the model to use to represent the relationship between the median sediment grain size and the backscattering coefficient from the SAR data. The reasoning being, Wu et al., (2019) used a scatter plot in their study to display this relationship between the variables, and van der Wal et al., (2005) used linear regression models, as well as highlighting the fact that regression models have been successfully used in previous studies which have used optical remotely-sensed data to map sediment grain size, and cited Yates et al.,'s (1993) study, which used satellite imagery to classify the distribution of intertidal sediments, as an example of one of these studies which used regression models successfully.

2.4 Field Locations
2.4.1 East Coast
There are a lack of recent studies which specifically observe grain size and sediment transport across the East Coast of England, in the Norfolk and Suffolk region. Considering that, according to the 'Living on the Edge' insurance study, based on Environmental Agency data, the top two areas which were found to be most at risk of coastal erosion were Happisburg in Norfolk and Kessingland in Suffolk respectively (Living on the Edge [online], 2019), with Poulton et al., (2006) concluding that the cliffs at Happisburg eroded approximately 105 m in 12 years, from 1992-2004; then it is

highly reasonable to conclude that understanding of the grain size and transport in this area is imperative to minimise coastal erosion in this region.

An early study by McCave (1978) found that overall, sediments became coarser in the direction of the waves, from North to South along the East Anglian coastline. This is contradictory to general sediment transportation trends, as sediment usually gets finer in the direction of the waves (McCave, 1978), due to erosional processes, such as attrition. This is where sediment collide during wave transportation and become smaller and smoother in the process. The coarsening of sediment in the East Anglian region was attributed to the winnowing of sediment down shore and strong tidal currents by McCave (1978). Yet, despite this somewhat abnormal observation in the late-70s, limited academic work has been published since, which limits comparison. This is particularly problematic especially as coastal areas are highly dynamic.

2.4.2 Chesil Beach
Chesil Beach is a shingle barrier beach located in Dorset, in the South-West coast of England. It is geologically famous for its grading of sediment. Bird (1996) states that the pebble size on Chesil Beach is graded south-eastwards from small to large pebbles, coinciding with the increase of wave energy. The same grading pattern of sediment was also found previously by Carr (1969). This is abnormal, as the pebbles grade from small to large, going against the transportation direction and direction of longshore drift, opposite to what would be expected. This is attributed to the fact that attrition is a slow process, the south-west currents are very strong, enabling transportation of larger sediment, and that the longshore drift direction along this beach has alternated throughout history (Bird, 1996).

The grading of sediment at Chesil Beach has been studied for decades, but again, papers detailing the size and transport of sediment at Chesil Beach are dated; yet are still assumed to be relevant to date.

2.5 Beach Elevation and Gradient
The relationship between beach gradient and grain size has been studied for decades. Bascom (1951) found that a steeper beach gradient is indicative of coarser beach sediment. More recently, this relationship has been studied and confirmed by Bujan et al., (2019) and McFall (2019), amongst others. Therefore, as a result of this well-studied relationship, it can be hypothesised that beach slope can be used as a proxy to determine average grain size.

From a remote sensing perspective, as a result of this relationship, LiDAR data could potentially be used to determine grain size on beaches. LiDAR DTMs (Digital Terrain Models) can show the beach elevation and slope, and therefore may be able to estimate the grain size present on the beach. LiDAR return signal intensity (LRSI) has also been used in multiple studies, such as that by Long et al., (2006) which hypothesised a positive association between the LRSI and grain size, due to the established relationship as discussed above. Although the study did find some evidence of this, the amount of available data was too small to precisely quantify the relationship. A study by Burns (2019) found a strong correlation between the LRSI and coastal sediments. However, the conclusion was unexpected as a linear decrease in LRSI was found with increasing grain size, whereby the expectation was to find the reverse. One reasoning Burns (2019) used to explain this unexpected relationship was that based on the findings of Garestier et al. (2014), which state that additional factors, unrelated to sediment grain size, including sediment composition and colour can also have an influence on the LRSI. Recent studies have had better success in using LiDAR to analyse sediment grain size. A

study by Chardon et al., (2020) was able to estimate the grain size distribution and produce grain size maps in above-water areas in rivers, using LiDAR topographic surveys.

These studies demonstrate that it is highly probable that there will be a strong relationship between the beach gradient, the beach elevation and the sediment grain size on the beach and suggests that sediment grain size may be able to be derived from these values.

2.6 Remote Sensing

Recent studies using remote sensing methods to determine beach grain size have involved the use of optical imagery. Cabezas-Rabadán et al., (2021) studied whether shoreline variability, from Sentinel-2 optical images, was indicative of sediment grain size along beaches. They found promising results, concluding that high shoreline variability is indicative of finer grain sediment, and this variability decreases as the grain size becomes coarser. This was found to be accurate to an R^2 of 0.70 (Cabezas-Rabadán et al., 2021). However, optical imagery relies on areas being cloud-free to get good quality images. This study took place in Eastern Spain, it is probable that this area had more cloud-free days than the UK. Therefore, optical imagery from this area can be easily collected in contrast to over the UK. As previously discussed, radar remote sensing can collect data independent of weather, and will therefore provide a greater annual coverage than optical imagery. A benefit of this is that sediment changes can be observed on the beach after and during storm events, making the use of SAR data advantageous over the use of optical imagery for this application.

Other studies have looked at determining sediment grain size using various types of remote sensing equipment, not just satellite data. Lurton et al., (2015) found that backscatter from multi beam echo sounders directly relates to the sediment grain size. Similar to what has been found in the literature with regards to satellite SAR data, they found that this relationship is caused by the roughness and the hardness of the substrate, which are also directly correlated with sediment grain size.

2.7 Gaps in the Literature

Much of the literature agrees that traditional surveying techniques to determine sediment grain size are very time consuming, especially as coastal areas are highly dynamic environments (Chardon et al., 2020; Cabezas-Rabadán et al., 2021). Therefore, the use of remote sensing techniques to determine sediment grain size without the need for ground surveying are increasingly being studied.

There is no known study which predominantly focuses on investigating the relationship between SAR backscatter and grain size of beach materials in the UK. There is also no study which uses both C-band and S-band SAR for this application, allowing for a comparison between these two different SAR bands.

Despite the lack of literature in this area thus far, the need for quick beach surveying is apparent, due to the increased risk of erosion and storm surges, due to climate change. In addition to this, records and published literature on transportation and the grain size of sediments around UK coastlines are largely outdated, or non-existent. The use of SAR data provides an opportunity for quick beach surveying, independent of weather, for multiple areas across the UK to help tackle pressing issues, such as erosion.

It is hoped that this research will provide a foundation for studies into further investigating the relationship between SAR backscatter and grain size, both on beaches and other environments.

3. METHODOLOGY

3.1 Fieldwork Methodology

As part of this study, fieldwork investigations were conducted to obtain ground-truth data for sediment grain size and beach elevation. Fieldwork was carried out in May 2022. Five fieldwork sites with varied sediment size were surveyed across England. Sediments were classified according to the Wentworth (1922) Particle Size Scale (Appendix A). A map of the field locations is shown in Figure 5.
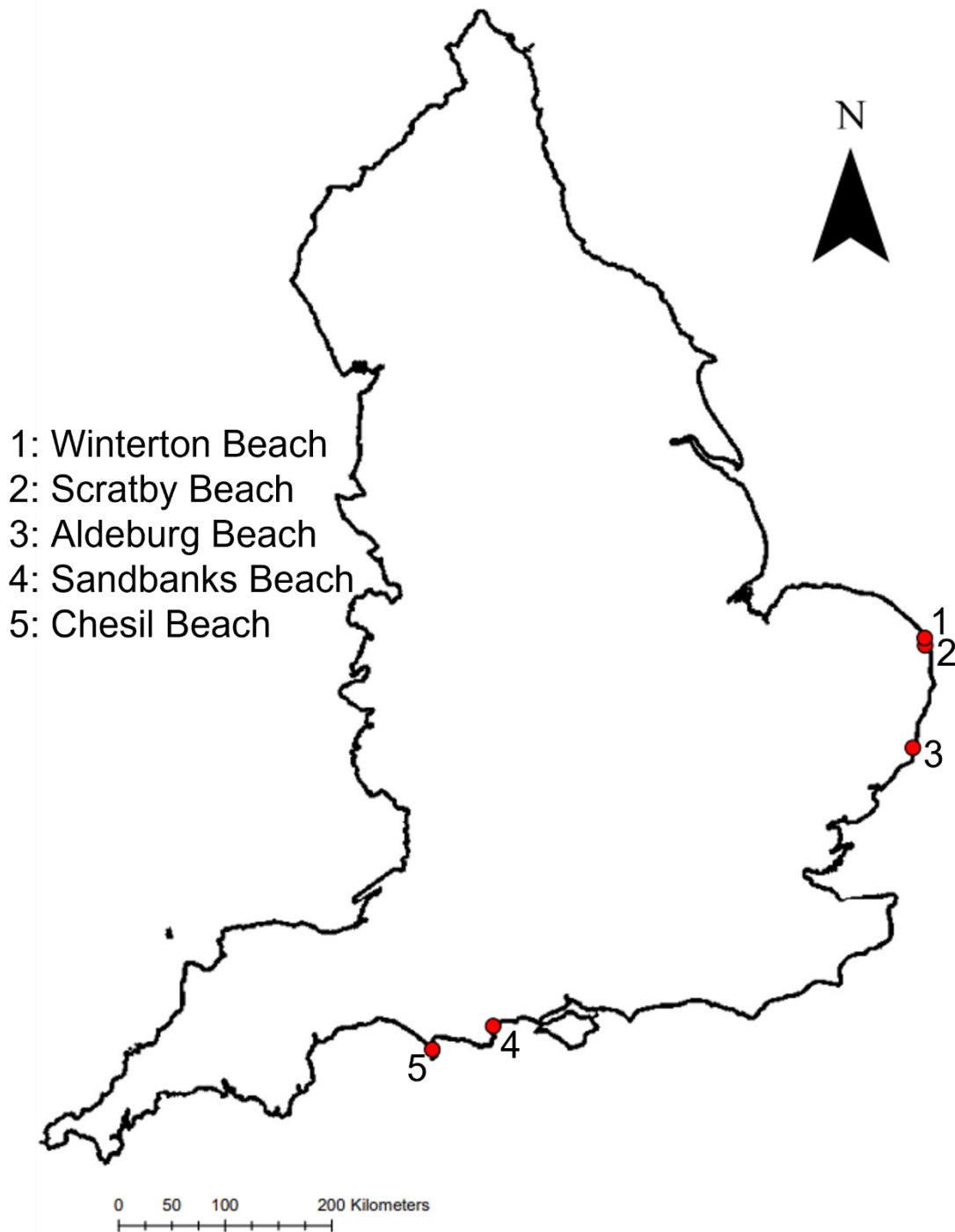
Figure 5: A map of England showing the locations of the study sites.

3.2 Study Sites

The five study sites surveyed were as followed:

- Chesil Beach, Dorset, South-West Coast of England – 4 sediment samples taken at each location for 5 locations along the beach from West Bay to Portland – sediment ranged from granule stones to cobbles.
- Sandbanks Beach, Dorset, South-West Coast of England – 7 sediment samples taken randomly at 3 locations along the beach from Cubs Beach to Canford Cliffs Beach – sediment was fine to medium sand.
- Aldeburgh Beach, Suffolk, East Coast of England – 3 sediment samples taken at each location for 3 locations along the beach at Slaughden, Aldeburgh Main Beach and Thorpeness – sediment was medium-sized pebbles.
- Scratby Beach, Norfolk, East Coast of England – 8 sediment samples taken along the beach from California to Scratby Beach – sediment was medium sand.
- Winterton Beach, Norfolk, East Coast of England – 6 sediment samples taken along the beach – sediment was medium sand.

Each cross-section of the beach, where GPS and sediment measurements were taken, were given a site 'code', in which the sites will be referred to throughout this project, these are laid out below in Table 1.

Table 1: Fieldwork site codes with the start and end easting and northing coordinates, along with the median sediment size at each site. NB: Coordinates are in British National Grid.

Beach	Site Code	Start Easting	Start Northing	End Easting	End Northing	Median Sed. Size/ mm
Chesil Beach (Portland)	C1	368223.5	73682.2	368168.5	73639.9	64.7
Chesil Beach (Portland)	C2	368148.6	73821.6	368072.7	73756.6	61.8
Chesil Beach (Portland)	C3	368048.2	73939.8	367973.1	73870.3	61.7
Chesil Beach (Portland)	C4	367968.6	74070.5	367874.6	73979.0	54.5
Chesil Beach (Visitors Centre)	C5	366653.7	75476.8	366576.6	75411.1	37.2
Chesil Beach (Visitors Centre)	C6	366534.0	75596.7	366463.3	75528.7	37.5
Chesil Beach (Visitors Centre)	C7	366443.4	75727.6	366356.4	75643.3	37.4
Chesil Beach (Visitors Centre)	C8	366301.8	75791.7	366255.5	75748.1	33.6
Chesil Beach (Abbotsbury)	C9	355957.0	84601.2	355895.6	84525.2	20.1
Chesil Beach (Abbotsbury)	C10	355831.2	84693.6	355772.5	84615.2	17.3
Chesil Beach (Abbotsbury)	C11	355702.1	84764.7	355649.7	84702.0	18.6
Chesil Beach (Abbotsbury)	C12	355569.9	84848.2	355524.9	84790.5	17.2
Chesil Beach (West Bexington)	C13	353029.0	86522.8	352984.3	86451.1	13.1
Chesil Beach (West Bexington)	C14	352906.5	86603.5	352856.2	86534.1	12.3
Chesil Beach (West Bexington)	C15	352772.4	86693.4	352722.1	86620.4	10.6
Chesil Beach (West Bexington)	C16	352648.6	86766.3	352602.3	86699.3	8.9
Chesil Beach (West Bay)	C17	346276.4	90307.2	346255.4	90246.8	4.9

Chesil Beach (West Bay)	C18	346425.4	90259.4	346392.0	90186.0	4.9
Chesil Beach (West Bay)	C19	346546.4	90145.6	346533.9	90120.9	5.3
Chesil Beach (West Bay)	C20	346677.3	90075.6	346664.4	90052.7	5
Sandbanks Beach	SB1	403911.3	87084.33	403933.2	87062.21	0.213962
Sandbanks Beach	SB2	404043.3	87156.89	404053	87127.74	0.209696
Sandbanks Beach	SB3	404159.7	87248.08	404190.8	87210.93	0.267522
Sandbanks Beach	SB4	404265.6	87351.64	404294.3	87321.58	0.247889
Sandbanks Beach	SB5	404846.8	88094.51	404878.4	88063.9	0.579671
Sandbanks Beach	SB6	405491.1	88817.48	405532.6	88775.77	0.296486
Sandbanks Beach	SB7	405827.1	89127.12	405872.2	89072.22	0.312953
Aldeburgh Beach (nr. Slaughden)	A1	646390.4	255485.9	646421.6	255481.1	36.3
Aldeburgh Beach (nr. Slaughden)	A2	646411.3	255633.1	646448.1	255629.6	31.4
Aldeburgh Beach (nr. Slaughden)	A3	646434	255785	646473.4	255776.3	36.2
Aldeburgh Beach (central)	A4	646509	256328.7	646574	256317.2	37.4
Aldeburgh Beach (central)	A5	646525.7	256471.7	646599.8	256460	38.2
Aldeburgh Beach (central)	A6	646552.8	256620.9	646628.8	256609.6	30.3
Aldeburgh Beach (Thorpness)	A7	647304.9	259513.3	647357.8	259492.1	30.9
Aldeburgh Beach (Thorpness)	A8	647370.5	259645.4	647412.9	259627.9	36.3
Aldeburgh Beach (Thorpness)	A9	647431.3	259783	647471.8	259768.7	39.3
Scratby Beach	S1	651755.9	314940.1	651805.8	314963.3	0.340788
Scratby Beach	S2	651696.6	315063	651753.3	315089.1	0.371085
Scratby Beach	S3	651643.5	315186.8	651704.8	315213.0	0.354982
Scratby Beach	S4	651591.8	315303.7	651656	315332.5	0.363372
Scratby Beach	S5	651536.4	315422.8	651606.4	315454.2	0.35086
Scratby Beach	S6	651495.7	315540.2	651554.2	315576.6	0.345675
Scratby Beach	S7	651446.9	315665.5	651503.8	315687.3	0.355156
Scratby Beach	S8	651396.7	315777.1	651457.5	315800.3	0.359893
Winterton Beach	W1	649888.0	319683.8	649937.7	319702.4	0.444309
Winterton Beach	W2	649849.5	319827.4	649891.8	319841.2	0.334048
Winterton Beach	W3	649796.2	319973.9	649866.5	319979.8	0.36413
Winterton Beach	W4	649793.9	320116.8	649865.8	320134.5	0.404789
Winterton Beach	W5	649742.5	320264.4	649867.7	320299.1	0.361047
Winterton Beach	W6	649698	320403.7	649770.3	320451.4	0.458355

These locations were chosen to compare beaches in two different areas in England; Dorset and the East Coast and due to their graded sediment, i.e., Chesil Beach is a famous tombolo which has graduated sediment grain size from small pebbles at West Bay to large pebbles at Portland (Figure 6). Sandbanks Beach is also located in Dorset, but it consists of fine sand. This location is a small peninsula and therefore was chosen as a 'sandy' comparison to Chesil Beach, as although it is not a tombolo, the beach stretches out into the sea.

On the East Coast, Aldeburgh in Suffolk was chosen due to the presence of medium-sized pebbles, two additional adjoining sandy beaches were chosen in the East Coast, Scratby and Winterton Beach to provide a comparison between beaches with pebbles and sand within the East Coast. All the field sites do not have cliffs present, except for Scratby Beach. This is because the presence of cliffs is thought to result in increased double-bounce radar scattering. Scratby Beach was chosen despite the presence of cliffs, so that the double-bounce scattering effect can be evaluated, and compared to Winterton Beach, a sandy beach nearby without cliffs present.
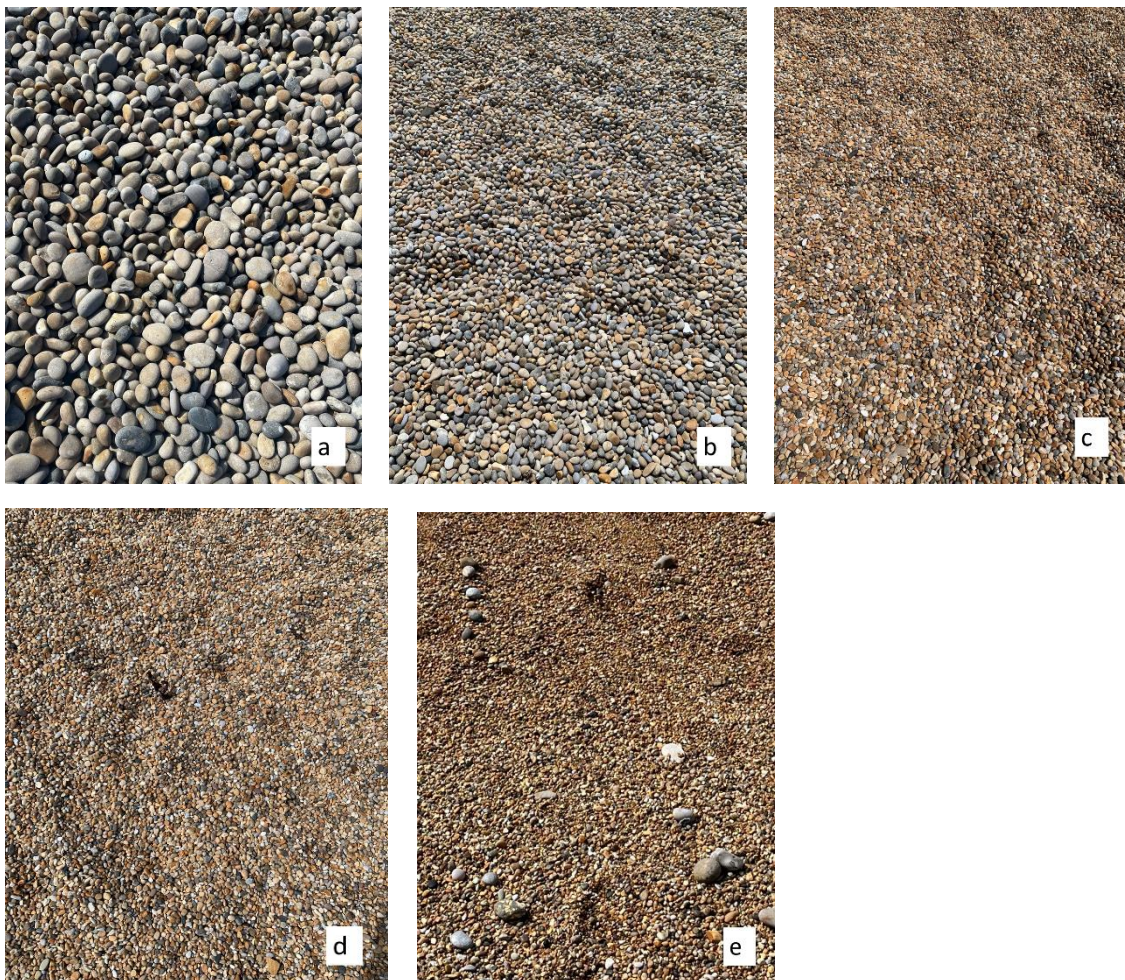
Figure 6: Sediment grading at field locations along Chesil Beach. a. Portland (Sites C1-C4), b. Chesil Beach Visitor Centre (C5-C8), c. Abbotsbury (C9-C12), d. West Bexington (C13-C16), e. West Bay (C17-C20).

Figure 7: Satellite Sentinel-2 Imagery of the five study areas. a. Chesil Beach, b. Aldeburgh Beach, c. Scratby and Winterton Beach, d. Sandbanks Beach. Imagery Date: 17/08/2022. Source: SentinelHub, (2022).

3.3 Beach Elevation Measurements

Beach elevation measurements were taken in the field using a *Leica GS10* GNSS receiver with a *CS10 controller*. The GNSS receiver was mounted onto a 2 m pole, with a rounded base (to prevent sinking into the sand and inaccurate measurements) (Figure 8). The RTK (Real Time Kinematic) system was used, to receive ground GNSS corrections from a base station or local network. This was achieved by receiving these RTK corrections over the 3G network. Receiving these RTK corrections meant that positional accuracy was reduced to within 2 cm. The x and y coordinates for the GNSS measurements were taken in British National Grid. The z coordinates recorded the elevation above sea level in metres (m).

Figure 8: Images of the *Leica GS10* GNSS receiver with a *CS10 controller* and rounded base used in the field.

Elevation measurements were taken along a cross section of the beach, from the back of the beach (backshore), to where the beach meets the sea (braker zone), perpendicular to the waterline. No set distance was specified, but measurements were taken regularly or when there was a notable change in beach elevation.

Cross-sections of the beaches, displaying beach profile were produced using the Python package 'Plotly'. This was done by calculating the cumulative distance, with the first coordinate recorded for the beach cross-section starting at 0, between the consecutive x and y coordinates and plotting these against the recorded beach elevation, z coordinate.

When calculating the gradient of the beach to compare to sediment size, the beach elevation in metres above sea level was plotted against the distance between the GNSS point with the highest point on the beach and the last GNSS point. The point with the highest elevation was used as some of the beaches had a slight flattened area with a promenade or footpath with a lower elevation, and therefore this was not considered the 'true' elevation. From this plot, the gradient of the line of best fit between the points were taken to represent the average gradient of the beach.

3.4 Sediment Sampling

At each location, sediment samples or surveys (for pebbles) were taken every 150 m either consecutively along the beach or at various points along the beach, depending on the length of the area surveyed.

As discussed, fieldwork methodology was based on the methodologies by van der Wal et al., (2005), van der Wal and Herman (2007). Sediment sampling and selection was based on the Wolman's (1954) pebble count method. In both cases, on sandy and stony beaches, sediment was sampled from the dry areas on the beach, so as not to be affected by moisture from the sea.

At stony beaches, sediments were measured in-situ. This is so that no pebbles were removed from the beach. This is especially important for Chesil Beach, which is a Site of Special Scientific Interest (SSSI) and a World Heritage Site, so removing pebbles is prohibited. The length, width, and depth of 25 randomly selected pebbles from along the cross-section were measured at each cross-section transect to give an overview of sediment size in the area. Measurements of the pebbles were taken using digital calipers with a resolution of 0.1 mm and accuracy of ±0.2mm.

At sandy beaches, 2x teaspoons of sand (approximately 10 cm³) was collected and placed in separate labelled plastic zip-lock bags. Sediment was needed to be removed

from sandy beaches as measurements cannot be taken in-situ without lab machinery, however a minimal amount of sediment was removed to limit the impact. Upon the end of the project, sediment will be returned to the beach area in which it was collected.

In the laboratory, 0.5 g of sandy sediment was weighed out and sediment grain size was measured using a *LS 13 320 Laser Diffraction Particle Size Analyzer* (Figure 9)*.* Obscuration of the sample in the machine ranged between 8-12 % for each sample.

For analysis, the median diameter of the sediment was calculated and used for comparison to the SAR backscatter. The median average was chosen as this average is less susceptible to outliers, such as a big or small pebble, which is not representative of the beach area as a whole. Wu et al., (2019) also used the median diameter of the sediment grain size to compare to mean backscattering coefficient in their study.

Figure 9: The *LS 13 320 Laser Diffraction Particle Size Analyzer* used to determine sand sediment grain size.

The overall field methodology explained above is concisely displayed in the flow diagram below (Figure 10).
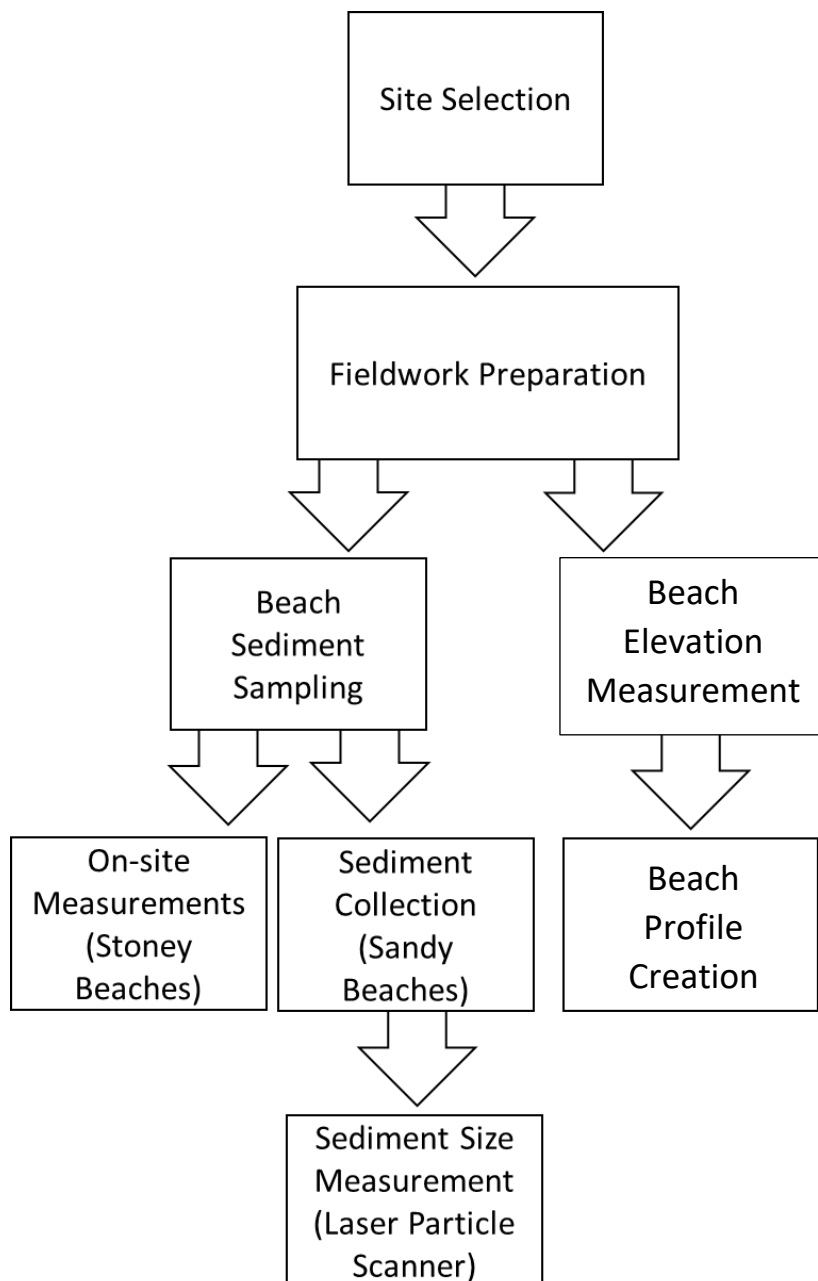
Figure 10: A flow diagram outlining the field methodology.

3.5 SAR Data Selection

The SAR data downloaded was acquired in May and June 2022, as this is closest to when fieldwork was carried out. Sentinel-1 data were downloaded from the Copernicus Open Access Hub and NovaSAR data were downloaded from the SEDAS portal. The three field locations on the East Coast (Aldeburgh, Scratby and Winterton) and the two field locations in Dorset (Chesil and Sandbanks) were displayed in the same images respectively for Sentinel-1 data. Images for each of the two main areas had as similar acquisition dates as possible. Two Sentinel-1 images and one NovaSAR for each of the field locations were selected as NovaSAR data was taken less regularly. There was no NovaSAR data available for Sandbanks beach. The file names for the SAR data used are as follows:

Dorset:

S1A_IW_GRDH_1SDV_20220507T062343_20220507T062408_043101_0525A2_7428

S1A_IW_GRDH_1SDV_20220522T175747_20220522T175812_043327_052C88_0B7A

NovaSAR_01_34304_grd_13_220531_101529_VV

East Coast:

S1A_IW_GRDH_1SDV_20220509T060647_20220509T060712_043130_0526A0

S1A_IW_GRDH_1SDV_20220521T060648_20220521T060713_043305_052BDF_9782

NovaSAR_01_35109_grd_13_220626_093326_VV (Aldeburgh)

NovaSAR_01_34652_grd_13_220611_225359_VV (Scratby and Winterton)

Details of the SAR data and the conditions present at the acquisition time were recorded (Table 2).

Table 2: Conditions at the time of SAR data acquisition. Data Sources: SAR Data: Sentinel-1 and NovaSAR Product Metadata. Weather and Wind Data: Time and Date, (2022). Tidal Data: Tide Times, (2022).

Location	Satellite	Acquisition Date and Time	Description	Weather Conditions	Wind Speed / mph	Wind Direct.	Tidal Stage	Pass	Angle of incidence near / °	Angle of incidence far / °
Dorset	Sentinel-1	07/05/22 07:09:04	Sentinel-1 IW Level-1 GRD Product	Overcast	13.05	N	In	Desc.	30.12	46.11
Dorset	Sentinel-1	22/05/22 17:56:44	Sentinel-1 IW Level-1 GRD Product	Mild and Sunny	4.35	SE	Low Tide	Asc.	30.23	45.97
Dorset	NovaSAR	31/05/22 10:15:30	6m Stripmap	Overcast	13.67	W	Out	Asc.	18.98	20.88
East Coast	Sentinel-1	09/05/22 06:58:01	Sentinel-1 IW Level-1 GRD Product	Mild and Sunny	8.08	S	Out	Desc.	30.08	46.07
East Coast	Sentinel-1	21/05/22 06:56:43	Sentinel-1 IW Level-1 GRD Product	Slightly Cloudy	8.70	W	Out	Desc.	30.08	46.07
East Coast (Aldeburgh)	NovaSAR	26/06/22 09:33:27	6m Stripmap	Slightly Cloudy	13.05	SSW	In	Asc.	19.06	20.94
East Coast (Scratby and Winterton)	NovaSAR	11/06/22 22:54:00	6m Stripmap	Slightly Cloudy	9.32	WSW	Out	Desc.	18.09	19.98

3.6 Tidal Data

In depth tidal data with the exact tide height for each location at the times of SAR data acquisition are displayed in Table 3 below.

Table 3: Tidal data for each location at the acquisition date of the SAR data. Data Source: Tide Times (2022).

Location	Date	Time	High/Low	Tide Height/ m
Chesil	07/05/22	04:21	Low	1.32
		11:07	High	3.18
		16:32	Low	1.51
		23:11	High	3.39
Sandbanks	07/05/22	08:13	Low	1.05
		17:24	High	1.92
		20:34	Low	1.40
		23:55	High	1.67
Aldeburgh	09/05/22	06:28	High	2.16
		10:53	Low	1.36
		17:39	High	2.30
Scratby and Winterton	09/05/22	02:34	High	2.39
		07:59	Low	1.66
		13:44	High	2.60
		21:38	Low	1.16
Chesil	22/05/22	00:01	High	3.40
		05:32	Low	1.23
		12:45	High	3.01
		17:44	Low	1.52
Sandbanks	22/05/22	02:26	High	1.82
		09:23	Low	0.83
		18:45	High	2.02
		22:07	Low	1.20
Aldeburgh	21/05/22	03:32	High	2.67
		09:15	Low	0.88
		15:33	High	2.65
		22:02	Low	0.36
Scratby and Winterton	21/05/22	06:21	Low	1.18
		11:41	High	3.12
		19:08	Low	0.66
Chesil	31/05/22	01:21	Low	0.86
		08:07	High	3.63
		13:35	Low	0.87
		20:16	High	3.85
Scratby and Winterton	11/06/22	05:35	High	2.93
		11:59	Low	1.33
		17:18	High	3.08
Aldeburgh	26/06/22	03:38	Low	0.70
		10:27	High	2.56
		16:04	Low	0.93
		22:22	High	2.49

3.7 SAR Data Processing

Sentinel-1 and NovaSAR data is to be used in the project. These SAR satellites have different bands of C-band and S-band respectively. The SAR data are being analysed in SNAP; a software developed by ESA. To process NovaSAR data, a separate plug-in is required.

For Sentinel-1, the data was acquired from Sentinel-1A in 'GRD' product type and 'IW' sensor mode for VV and VH polarisations. VV polarisation was chosen as this is the polarisation in which van der Wal et al., (2005) used in their study, of which the methodology for this study is based upon. For NovaSAR, the 'GRD' product type was

used in VV polarisation, as VH polarisations were not available for the area and time of interest.

Outline of the processing methodology workflow of Sentinel-1 and NovaSAR data are shown in Figure 11.
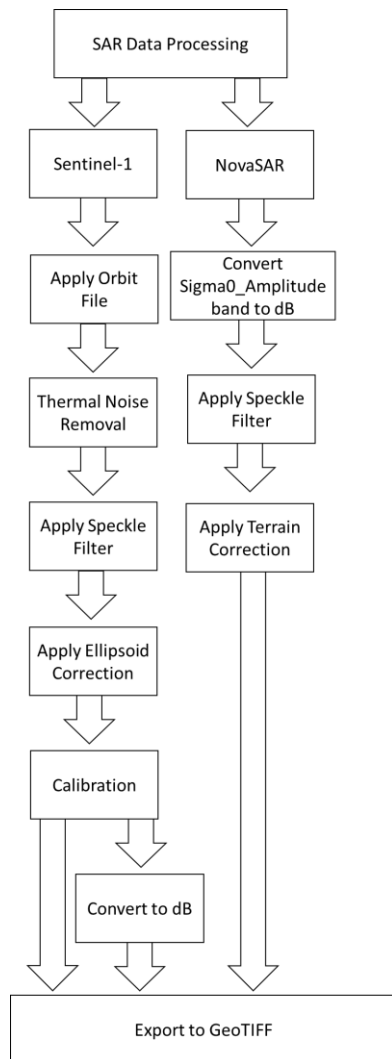
Figure 11: A flow diagram showing steps of SAR data processing.

For Sentinel-1 data, the same data processing was applied to both VV and VH polarisation. First, the data was subset, so that only the area of interest was displayed, to reduce processing time. This was followed by applying an orbit file to spatial coregister the data (UN SPIDER, 2022), the thermal noise from the imagery was removed, speckle filtering was carried out and an ellipsoid correction was applied, so that the SAR data has the correct geographic orientation. The data was calibrated so Sigma0 and thus, backscatter intensity was displayed. These calibrated images were then exported to separate GeoTIFFs for each polarisation. The calibrated images were then converted from backscatter intensity to dB units (backscatter coefficient), as the backscattering coefficient is widely used in the literature. σ° is converted to dB using the following equation:

$$dB = 10 * log_{10}(\sigma°)$$

After conversion, the dB bands for each polarisation were also exported to separate GeoTIFFs.

For NovaSAR data, the process followed was based on NovaSAR processing guidance provided by the UK Hydrographic Office (UKHO), who regularly work with NovaSAR data. Upon download, NovaSAR data is already calibrated and thus, already expressed in Sigma0. The Sigma0 band, which shows backscatter intensity had a speckle filter and terrain correction applied and then this processed data was exported to a GeoTIFF. The Sigma0 band was then converted to dB and underwent processing before being exported to a GeoTIFF.

3.8 QGIS Analysis

The exported Sentinel-1 and NovaSAR GeoTIFF files, for backscatter intensity and backscattering coefficient, were analysed in QGIS, a free, open-sourced GIS software.

For QGIS analysis, the GNSS points collected during fieldwork were converted to a shapefile and displayed in QGIS. This was to give the GeoTIFFs geographical reference of where sediment was measured from. For each of the GeoTIFF layers, i.e., Sigma0_VV, Sigma0_VH, dB_VV and dB_VH, raster layers encompassing a 30x100 m area (3x10 Sentinel-1 pixels, of which each pixel is 10 m x 10 m and 6x16 NovaSAR pixels of which each pixel is 6 m x 6 m) around each measure cross-section of the beach were extracted. Using the raster layer statistics tool, the mean intensity and dB for each raster were obtained.

3.9 Graphical Representation

To display the relationship between backscatter intensity and backscattering coefficient, scatter plots were used to plot median sediment size against the mean backscatter intensity and mean backscattering coefficient. The x axis on these graphs were converted to a logarithmic scale, as there was a big difference between the median sediment grain size of the sandy beaches and the stony beaches, so that all the data points could be displayed. As discussed, multiple previous studies used and suggested the use of regression models (van der Wal et al., 2005; Wu et al, 2019; Yates et al., 1993). A linear relationship was observed, and so a linear line of best fit was plotted.

As a linear relationship was observed, the correlation between the variables was calculated using the Pearson's Correlation Coefficient Equation (Figure 12). All of the tests were carried out at a 1 % significant level.

$$r = \frac{\sum (x_i - \bar{x})(y_i - \bar{y})}{\sqrt{\sum (x_i - \bar{x})^2 \sum (y_i - \bar{y})^2}}$$

Where,

r = Pearson Correlation Coefficient

x_i = x variable samples y_i = y variable sample

$\bar{x}$ = mean of values in x variable $\bar{y}$ = mean of values in y variable

Figure 12: Pearson's Correlation Coefficient Equation.

3.10 Unknown Area

To determine whether the sediment grain size on a beach can be derived from SAR backscatter data, a stony beach, Weybourne Beach, which has 'unknown' sediment grain size, was chosen. The area was chosen on the East Coast, so that the backscatter data can be derived from the same SAR images which were used to derive backscatter from Aldeburgh Beach, Scratby and Winterton Beach. Five random points on the beach were selected, each encompassing a 30x100 m area (3x10 Sentinel-1 pixels). The mean backscatter intensity (displayed in terms of Sigma0) and mean backscattering coefficient (dB) in both VV and VH polarisations from these areas were calculated in QGIS, as per the method above.

The values for mean backscatter intensity and mean backscatter coefficient were then averaged. The line of best fit equations from the graphs created using the data from the areas where the sediment grain size was known were rearranged to display the equation in terms of x (where x = median sediment grain size). The values for the mean backscatter intensity and mean backscatter coefficient were then inserted into the equations, so that estimates of the median sediment for the unknown area could be derived.

Further fieldwork was carried out after the predictions were made to collect ground truth data and determine the actual median sediment grain size for Weybourne Beach. The length, width, and depth of 125 pebbles were measured from 5 areas on the beach, which were spaced 150 m apart. The median average of these pebbles was then taken and compared to the predictions.

4. RESULTS

4.1 Sediment Size and Sentinel-1 C-band SAR
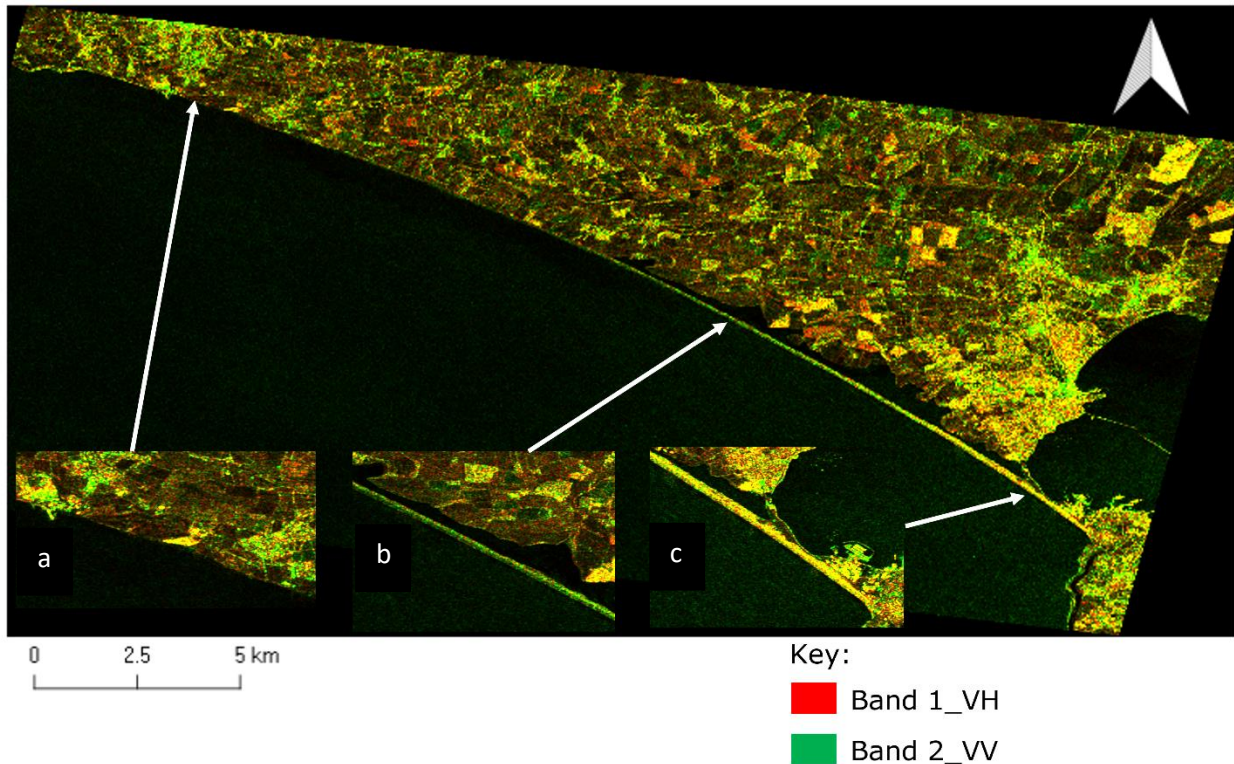
Figure 13: Observed backscatter from SAR imagery at Chesil Beach. (a) Backscatter at the top of Chesil Beach. (b) Backscatter at the mid-section of Chesil Beach. (c) Backscatter at the bottom of Chesil Beach.

Figure 13 shows the visual change in backscatter along Chesil Beach. At the top of Chesil, the SAR imagery is dim, representing a lower level of backscatter in both VH and VV polarisations (Figure 13a), the brightness of the imagery, and thus, amount of backscatter increases as you go south east along Chesil Beach, with the imagery becoming brighter in the mid-section of Chesil Beach (Figure 13b) and even brighter at the bottom of Chesil Beach (Figure 13c), showing a higher level of backscatter in both polarisations. This coincidences with a change in sediment grain size, graded from smaller to larger.

This brightness is quantified in the graphs below, using backscatter intensity and coefficient values from Chesil and the other beaches surveyed as part of this study.
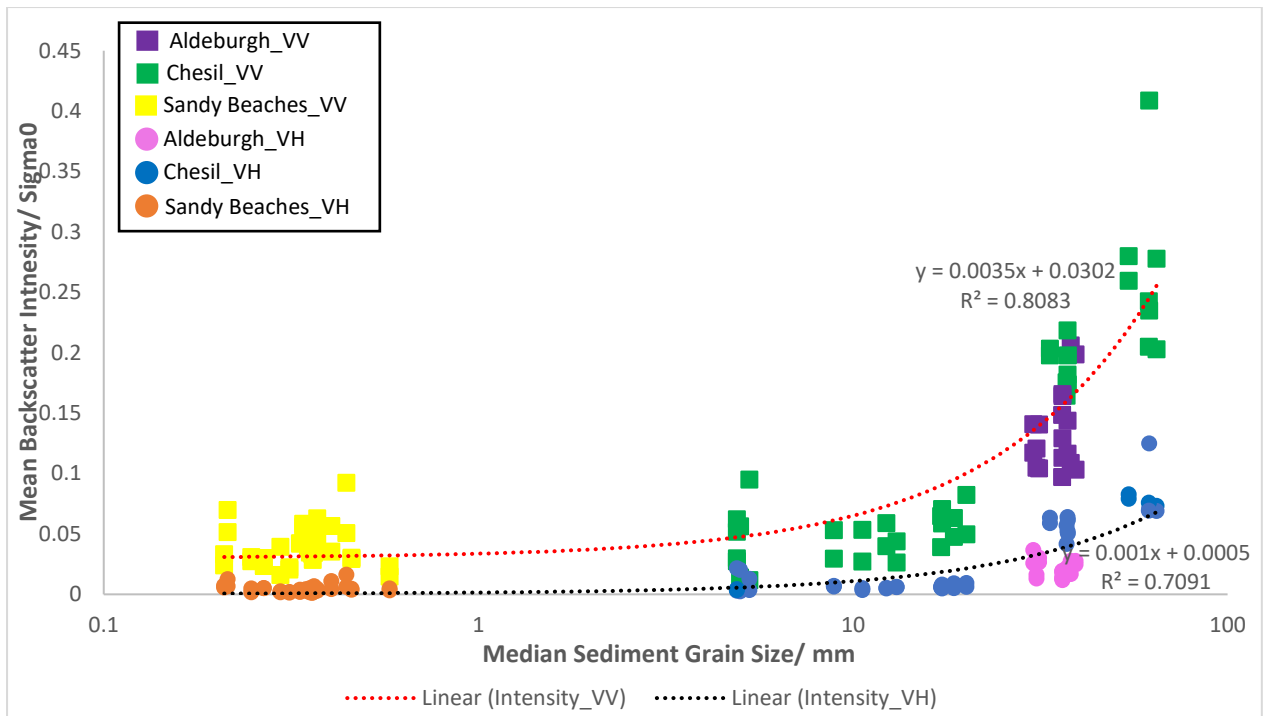
Figure 14: Mean backscatter intensity from Sentinel-1 data, displayed in Sigma0, plotted against median sediment grain size across all the field sites in which measurements were taken.
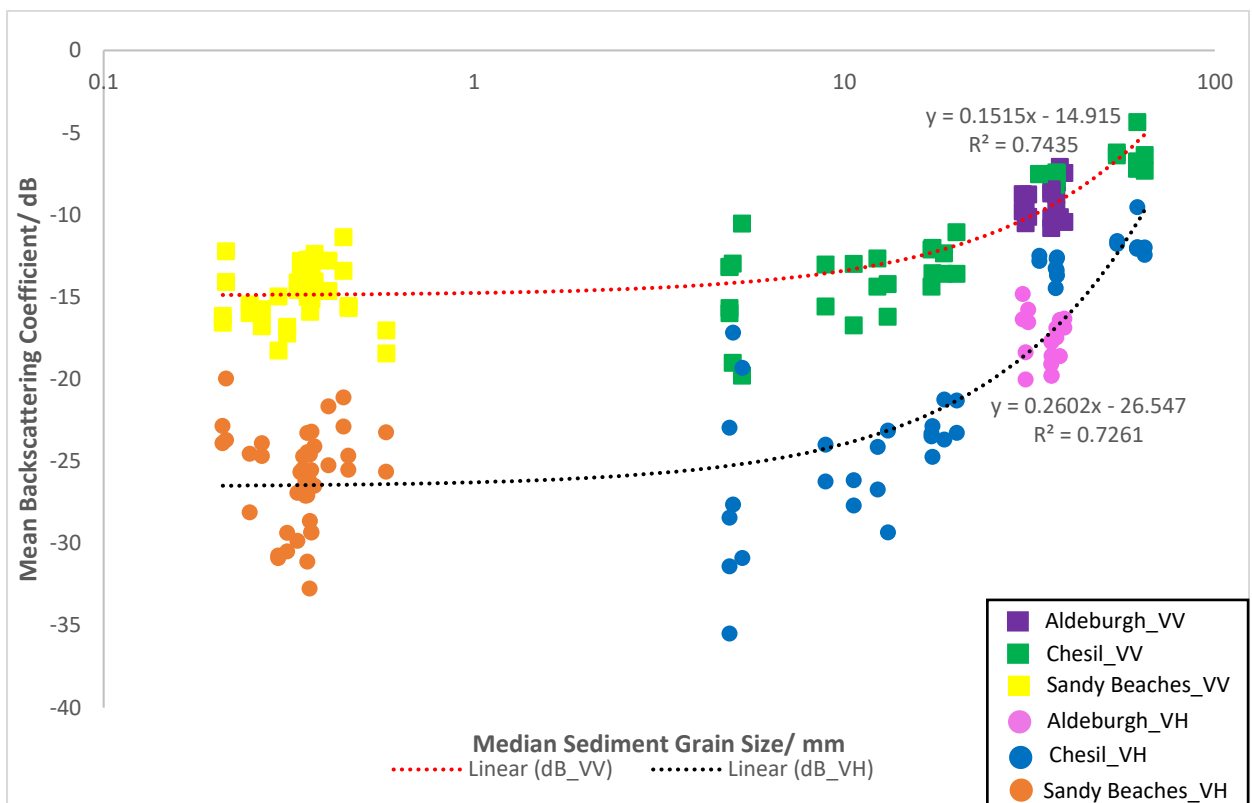
Figure 15: Mean backscattering coefficient (dB), from Sentinel-1 data, plotted against median sediment grain size across all the field sites in which measurements were taken.

When plotting the results from all the field sites onto one graph, there is a strong positive correlation between the backscatter intensity and the median sediment grain size in both VV and VH polarisations (Figure 14). The graph shows that the intensity is lower in the VH polarisation, compared to the VV polarisation, and the difference between these intensities gets larger as the median sediment size increases.

When calculating the Pearson's Correlation Coefficient for each of the polarisations, the correlation between sediment size and backscatter intensity for VV polarisation is $r(98) = 0.8991$, $p < 0.00001$, and for VH polarisation is $r(98) = 0.8421$, $p < 0.00001$, showing a very strong positive correlation between the variables in both VV and VH polarisations. R^2 values, which represents how well the data is fitted to the regression line, are 0.8083 and 0.7091 for the VV and VH polarisation respectively, which represents that the data fits the regression model well. The VV polarisation has a slightly higher value for both the Pearson's correlation coefficient and the R^2 value than the VH polarisation.

When the mean backscattering coefficient is plotted against the median sediment grain size, there is also a strong positive correlation, of $r(98) = 0.8623$, $p < 0.00001$ and $r(98) = 0.8521$, $p < 0.0001$, between the two variables, in VV and VH polarisations respectively (Figure 15). This graph shows that when the intensity values are converted to dB values, the backscattering coefficient is still higher in VV for all of the points, but that the difference between the mean backscattering coefficient between the VV the VH polarisation becomes smaller as the median sediment grain size increases.

The R^2 values for these lines of best fit are still high, of 0.7435 and 0.7261 for VV and VH respectively, showing that the data fits the linear regression line well.
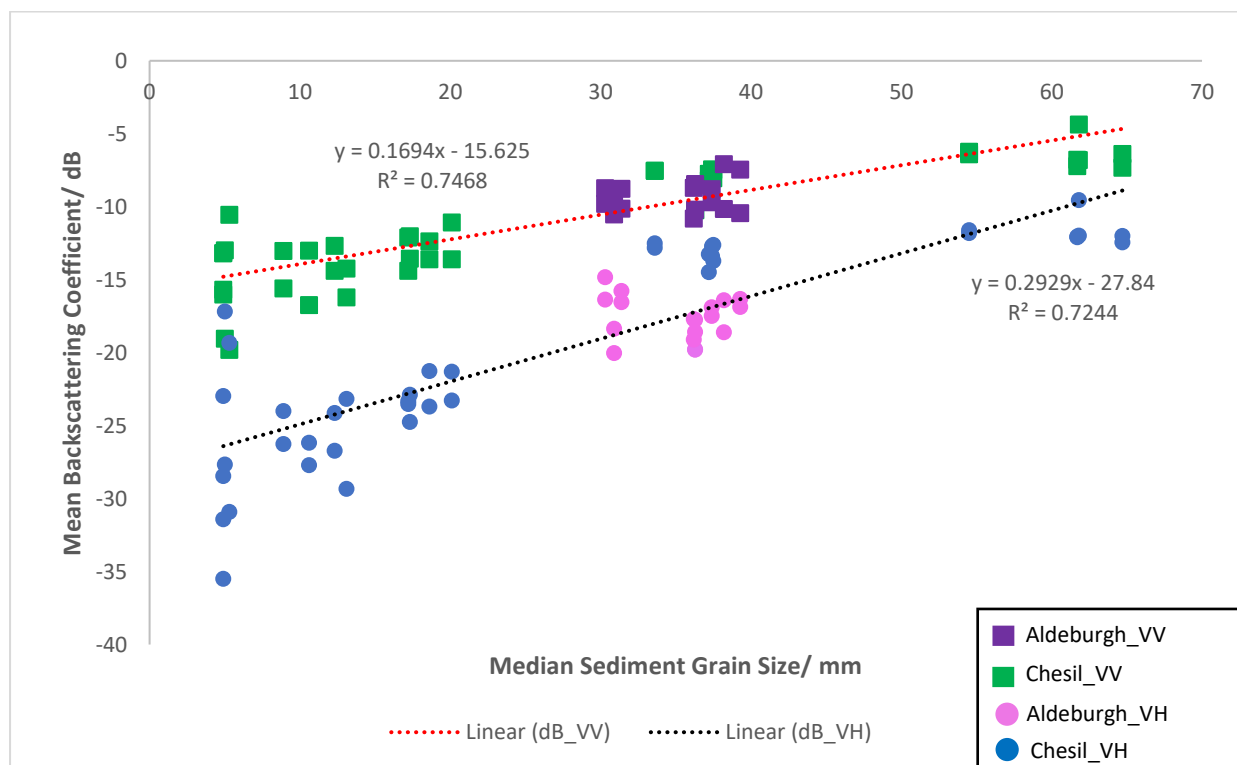
Figure 16: Mean backscattering coefficient plotted against median sediment grain size for stony beaches (beaches with sediment larger than 2 mm).
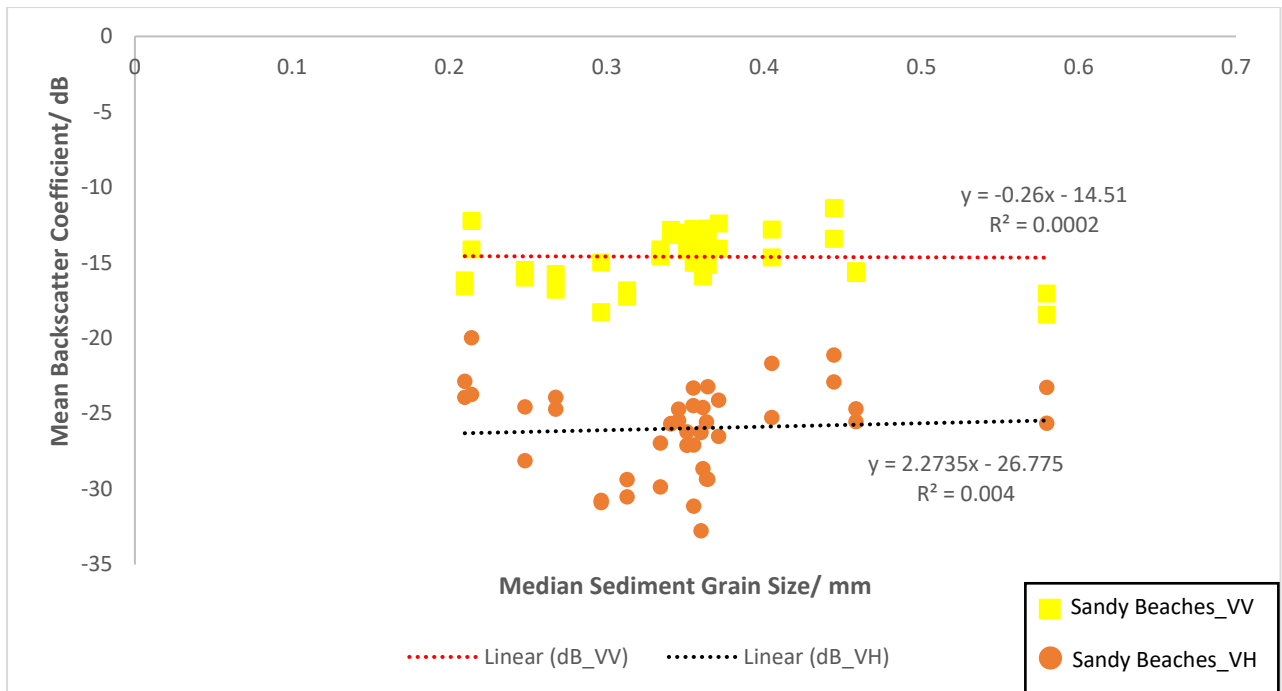
Figure 17: Mean backscattering coefficient plotted against median sediment grain size for sandy beaches (beaches with sediment smaller than 2 mm).

According to the Wentworth (1922) grain size classification, sediments between 0.0625 mm and 2 mm are classed as 'sand' and sediments larger than 2 mm are classed as 'gravel', therefore allowing us to split beaches in sandy beaches and stony beaches respectively. Upon splitting the data into these two categories, the relationship between sediment size and the backscattering coefficient varies.

For stony beaches, the Pearson's correlation coefficient still shows a strong positive correlation, of $r(56) = 0.8642$, $p < 0.00001$ and $r(56) = 0.8511$, $p < 0.00001$ and R^2 values, of 0.7468 and 0.7244, in VV and VH polarisations respectively (Figure 16). Again, the correlation and R^2 value is slightly higher in the VV polarisation compared to the VH.

However, for the sandy beaches, the Pearson's correlation coefficient is not significant, with a correlation coefficient of $r(40) = -0.0126$, $p > 0.939877$ in VV polarisation and $r(40) = 0.0633$, $p > 0.690446$ in VH polarisation (Figure 17), concluding that there is no correlation between the median sediment grain size and mean backscattering coefficient for sandy beaches. R^2 values for sandy beaches are also low for the lines of best fit for both polarisations, showing that the linear regression model does not fit the data on sandy beaches well.

4.2 Beach Elevation and Gradients

4.2.1 Beach Elevation
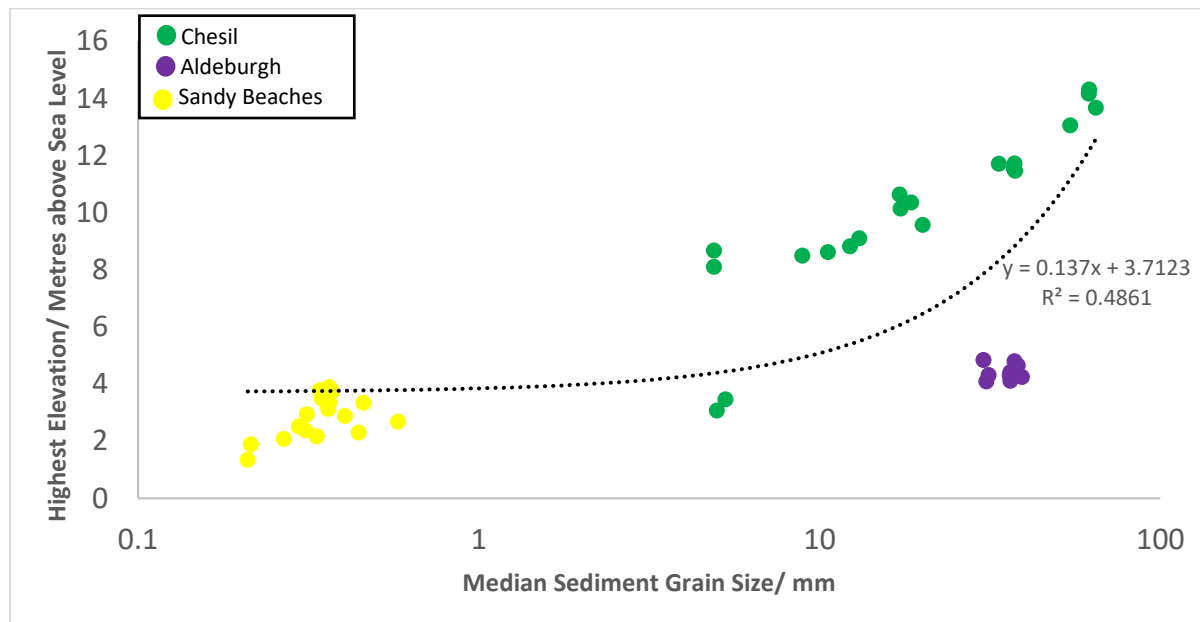
Figure 18: Highest elevation of the beach, measured in terms of metres above sea level, plotted against the median sediment grain size, in mm.

There is a moderate positive correlation between median sediment size and the highest elevated point on the beach (Figure 18). The Pearson correlation coefficient value between the two variables is $r(48) = 0.6972$, $p < 0.00001$ and the R^2 value is 0.4861, showing a relatively good fit to the linear regression model. However, despite having a moderate correlation, this varies between different beaches. For example, Aldeburgh beach has median sediment sizes ranging from 30.3 mm to 39.3 mm, but the highest elevations range for 4.09 m to 4.834 m compared to the range of 11.464 m to 11.72 m for sediment of the same size at Chesil Beach.

4.2.2 Beach Profiles

Beach profiles varied between different beaches and each section of the beach where fieldwork measurements were taken.
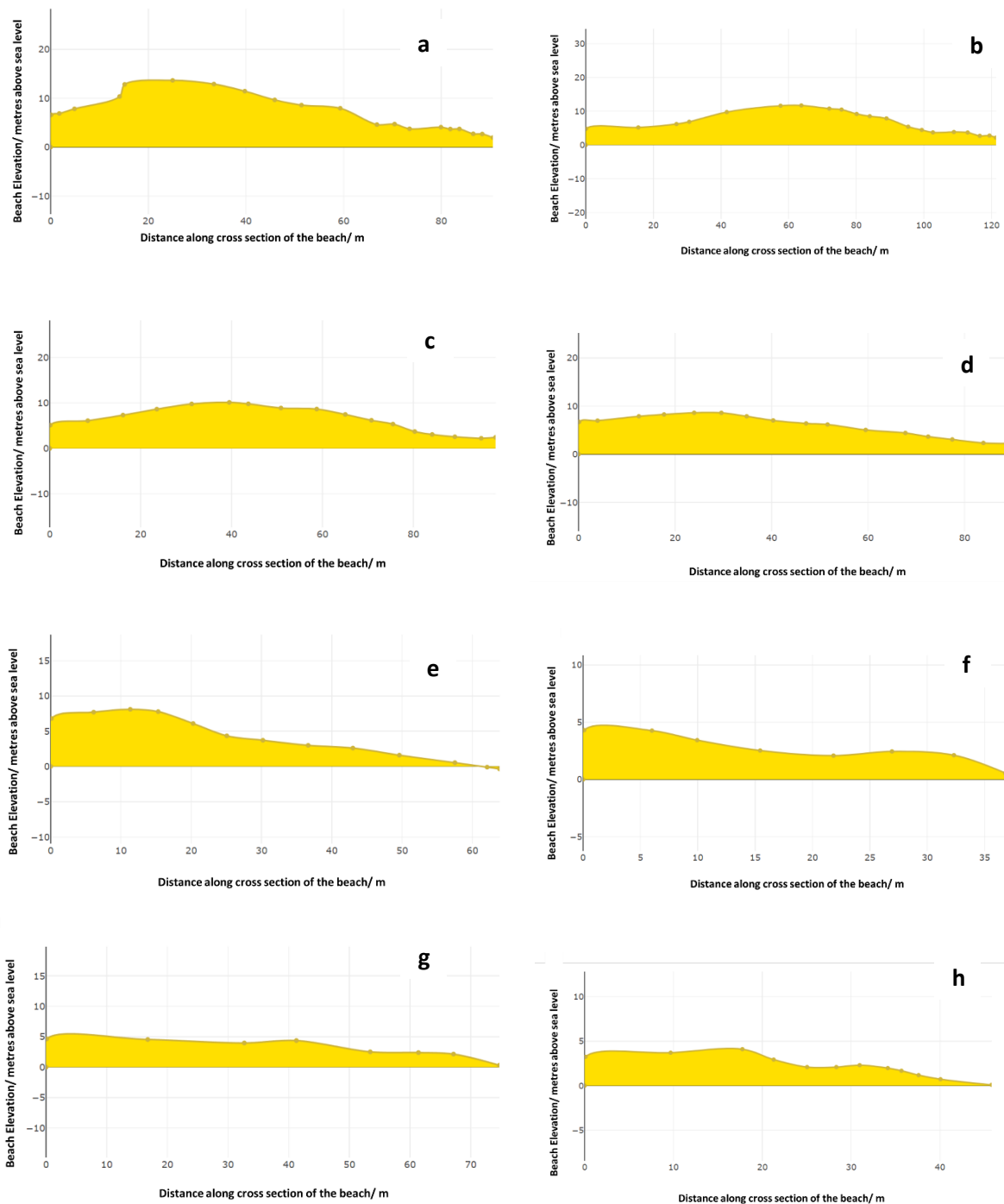
Figure 19: Beach profiles of field sites, detailing different sections of each stony beach. a. Site C2, Portland. b. Site C6, Chesil Beach Visitors Centre. c. Site C10, Abbotsbury. d. Site C15, West Bexington. e. Site C17, West Bay. f. Site A2, Aldeburgh, nr. Slaughden. g. Site A5, Aldeburgh, central. h. Site A7, Aldeburgh, Thorpeness.

The beach profiles display how the different beaches vary in both width of the cross section and the elevation above sea level (Figure 19).

At Chesil Beach, the beach profile varies as you go along the beach, which coincides with a change in the median sediment grain size. The beach profile near Portland, where median sediment size is 64.7 mm, shows a steep increase to an elevation of 13.669 m, with a gradual decline (Figure 19a). This is the highest elevation seen on any of the beach profiles. This then changes as you go along the beach (Figures 19b to 19e), wherby the elevation increase and then decrease for the other areas at Chesil Beach are more gradual and have a lower elevation above sea level overall.

The beach profiles for Aldeburgh Beach (Figures 19f to 19h) show that this beach has a lower starting elevation than the sites at Chesil Beach, with a more gradual decline in elevation. The starting elevation is most comparable to West Bay at Chesil Beach, which has a median sediment grain size of between 4.9-5.3 mm, yet this beach has a much steeper decline than at Aldeburgh, where the median sediment grain size varied between 30.3 – 39.3 mm.

Beach profiles for sandy beaches have a much lower elevation than at the stony beaches and a much more gradual decline.

4.2.3 Beach Gradients
To quantify this, a graph showing the mean average beach gradients plotted against the median sediment grain size is plotted below (Figure 20).
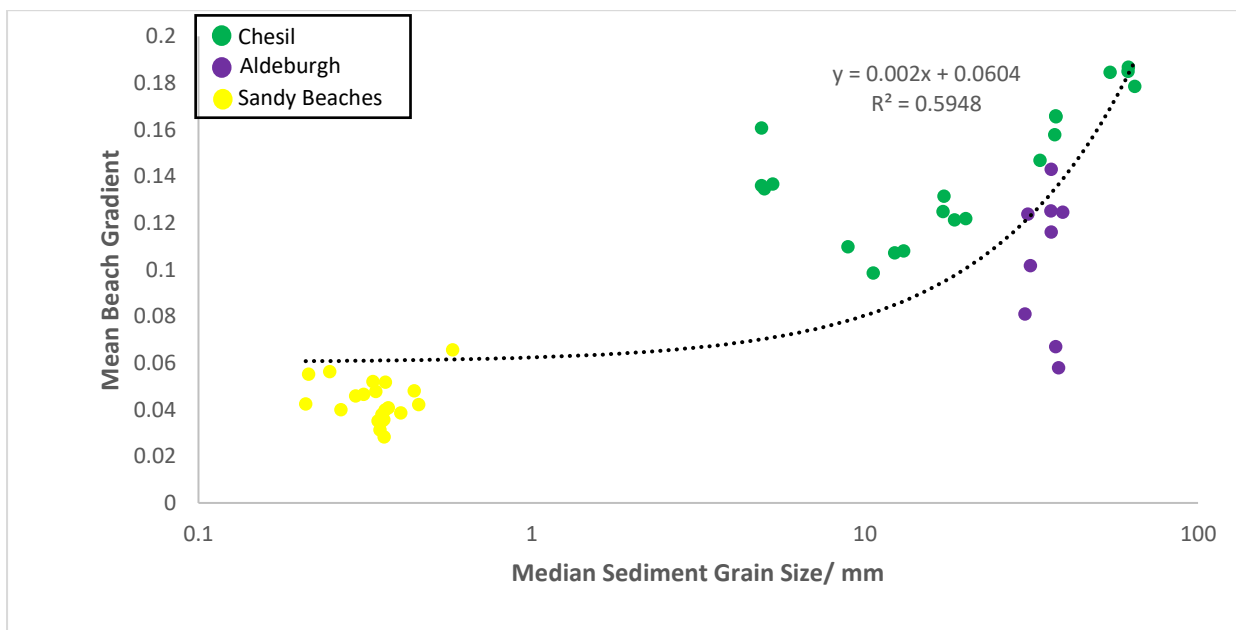
Figure 20: Average mean beach gradient plotted against the median sediment grain size across all field sites.

There is a strong positive correlation, of r(48) = 0.7712, p <0.0001, between the average gradient of the beach and the sediement size, with a general trend being as sediment size increases, so does the average gradient of the beach. However the R²

value, of 0.5948, shows that the line of best fit does not fit the data very well (Figure 20). As discussed from the beach profile analysis, most sites at Aldeburgh have a lower gradient compared to Chesil Beach, the other stony beach.

4.3 Sediment Size and NovaSAR S-band SAR
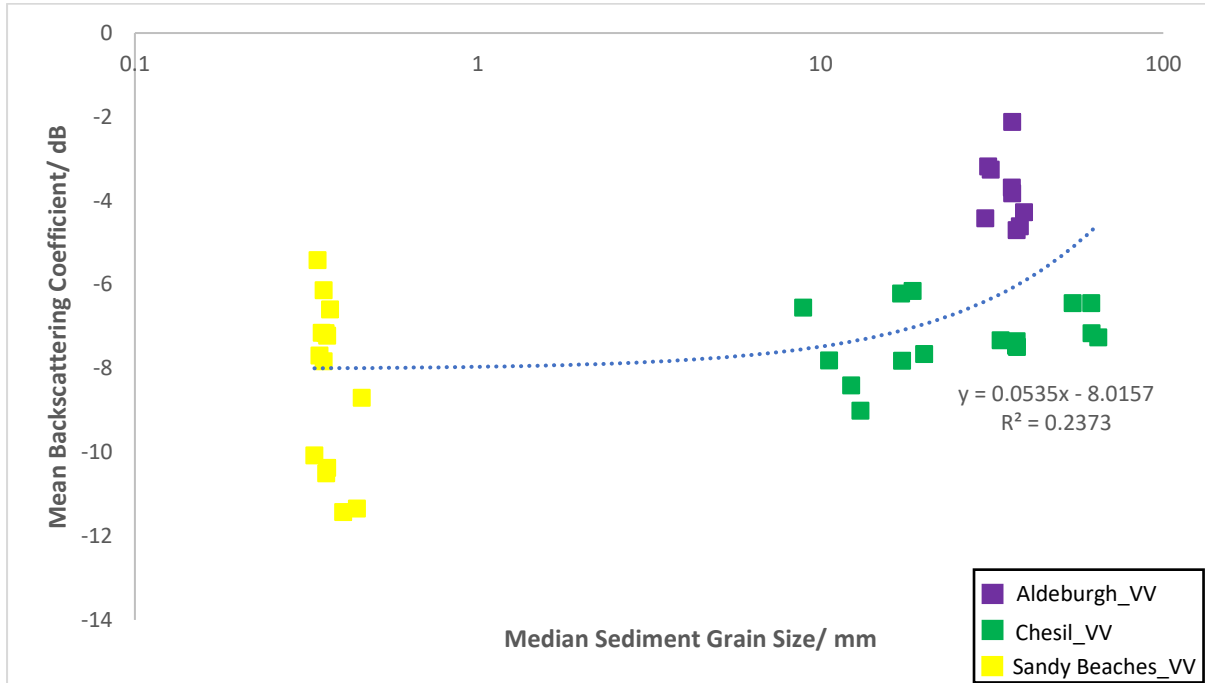
Figure 21: Mean backscattering coefficient from NovaSAR data in VV polarisation plotted against median sediment grain size for Chesil Beach, Aldeburgh Beach, Scratby Beach and Winterton Beach.

There is a moderate positive correlation of r(37) 0.4871, p <0.001662, between the median sediment grain size and the mean VV backscattering coefficient when looking at NovaSAR data. The R² value is 0.2537, showing that the linear line of best fit does not fit the data well (Figure 21).

When the correlation between the mean backscattering coefficient and the median sediment grain size is calculated from Chesil Beach alone, the beach with graded sediment, the correlation is not signifcant, with a Pearson's correlation coefficient of r(14)= 0.3227, p >0.260462, and a low R² value of 0.1042.

4.4 Unknown Area

To calculate a prediction for the median sediment grain size at an unknown area from the Sentinel-1 backscatter, the lines of best fit for both VV and VH polarisations in Figures 14 and 15 were used to input the respective backscatter values (Table 4).

Table 4: A table displaying the polarisation mode, the value inputted into the linear regression model and the predicted mean sediment grain size value output. NB: The predicted value is a mean average taken across 5 sites.

Polarisation	Intensity or Coefficient	Predicted value/ mm
VV	Intensity	36.61193
VH	Intensity	19.10898
VV	Coefficient	44.39872
VH	Coefficient	36.08606

The median sediment grain size at the area with unknown sediment size was found to be 33.44 mm. This is closest to the predicted value using the line of best fit from the VH coefficient values and then from the VV intensity values in Figures 15 and 14 respectively.

5. DISCUSSION

5.1 Sediment Size and Sentinel-1 C-band SAR

The results show a strong correlation between the median sediment grain size and backscatter intensity in both VV and VH polarisations, with a slightly greater correlation in VV polarisation compared to VH (Figure 14). There was also a strong correlation found between the mean beach backscattering coefficient and the median sediment grain size in both polarisations, again this being slightly higher in VV than VH (Figure 15). This agrees with the findings of Wu et al., (2019) and van der Wal et al., (2005), who also found a strong correlation between the mean beach backscattering coefficient and the median sediment grain size.

When the sediments were split into stony sediments (those with a diameter above 2 mm) and sandy sediments (those with a diameter below 2 mm), the results show that there is a strong correlation between stony sediments and the backscattering coefficients. Yet, no correlation was found between sandy sediments and the backscattering coefficients. This suggests that only larger sediments have an influence on the radar backscatter. Sentinel-1's wavelength ranges from 38 – 75 mm (Herndon et al., [online], 2019), and it is expected that this radar signal will interact best with objects that have the same, or larger, spatial magnitude than the wavelength (Rosenqvist et al., 2018). Therefore, it can be expected that larger pebbles will interact best with the radar signals. As the minimum range of the wavelength is 38 mm, it may be hypothesised that pebbles below 38 mm will not interact with the radar signals. However, Figure 16 shows a clear linear relationship between the median sediment grain size and the mean backscattering coefficient, despite some of the sediment being below 38 mm. This provides some evidence that smaller pebbles may interact with radar signals. However, it is possible that this variation in backscatter could be attributed to other factors, such as surface roughness on these beaches, therefore, further research into this is required.

There is no correlation between the median sediment grain size of sand and the mean backscattering coefficient, with the Pearson's correlation coefficient value not found to be statistically significant. Despite these findings, van der Wal et al., (2005) found a significant positive correlation whilst studying sediment with a grain size of up to 1 mm. However, this study attributed this variation mainly to surface roughness, caused as a result of the grain size. It can therefore be concluded that, as there is no correlation and a low R^2 value between the sediment size and the backscattering coefficient, that SAR C-band radar will not be able to be used to accurately measure the sediment size of sand on beaches. This is more than likely because grains of sand are just too small to be able to distinguish the different sizes of them using radar data. The grains of sand have a range of just 0.37 mm between the biggest and smallest sand grain size, and require a laser particle machine to measure them, hence cannot be measured by hand.

Upon comparing the graph in Figure 15 (all the field sites, including sandy beaches), and Figure 16 (just the stony beaches), the correlation between the mean backscattering coefficient is slightly improved when you exclude the data of sandy sediment in the VV polarisation, but it is slightly worse in the VH polarisation. However, the overall difference between these correlations when you include or exclude the sandy beaches in both polarisations is minimal. This suggests that the addition of sandy beaches into the results makes the model neither worse, nor better.

5.2 Effects of Polarisation and Surface Roughness

The backscattering coefficients in the VV polarisation are greater than those in the VH polarisation for all the data points. This agrees with Wu et al., (2019)'s findings who also found a greater mean backscattering coefficient under co-polarisations, in VV and HH, compared to cross-polarisations, in VH and HV. According to Woodhouse (2006), co-polarisations, such as VV polarisations are associated with smoother surfaces, whereas cross-polarisations, such as VH polarisations are associated with rougher surfaces. Based on this, as the VV polarisation signals are greater than the VH polarisation signals, it could be suggested that beach surfaces are relatively smooth. However, as the sediment size increases, so does the VH backscattering coefficient. This suggests that as sediment size increases, the beach surface becomes rougher. The SAR image is also brighter and has a higher overall backscatter intensity where sediment is bigger, which is one of the indicators of a greater amount of surface roughness in this area (Liew [online], 2001; Alaska Satellite Facility, 2022). This can be shown by analysing the beach profiles of beaches with bigger sediment, which show a greater variation in elevation (i.e., showing increases and then decreases in elevation), than beaches with smaller sediments (Figure 19).

In a VV polarisation, sediment within the 30-40 mm range at both Aldeburgh and Chesil have less of a difference in dB values than these two beaches do in VH polarisations. Meaning that from the graphs in Figures 15 and 16, these beaches are most distinguishable in VH polarisations than in VV polarisations. As discussed in further detail below, Chesil Beach has a rougher surface than Aldeburgh Beach, due to a greater elevation change, despite having a similar sediment size. As VH polarisation is more sensitive to surface roughness (Woodhouse, 2006), this explains why sites at Aldeburgh Beach have a lower backscattering coefficient in VH polarisation than VV polarisation compared to Chesil Beach. Nevertheless, the limited difference in the VV backscattering coefficient between Aldeburgh Beach and Chesil Beach, which have similar sediment size and a different roughness, (observed from the beach profiles in Figure 19), suggests the VV polarisation is somewhat responding to the actual sediment grain size and not just the roughness of the beach.

When the dB values are plotted, the line of best fits converge as the median sediment size increases (Figure 15). From the line of best fit equations, it can be predicted that the lines will cross, and the backscattering coefficient values in VH polarisation will become greater than VV polarisation, when the median sediment grain size reaches 107.01 mm. This is potentially due to the surface of areas that have bigger sediment size being rougher, which is a general trend that has already been observed in this study.

5.3 SAR Scattering Mechanisms

As discussed above, the backscattering coefficients are greater in VV polarisation than VH polarisation, showing a stronger co-polarisation return signal. As all the beaches are also orientated perpendicular to the SAR sensor, these two factors display the characteristics of direct backscattering (Rosenqvist et al., 2018), suggesting that this is the dominate scattering mechanism present. Alternatively, strong co-polarisation is suggestive of forward scattering, due to the smooth surface deflecting the signal away (Rosenqvist et al., 2018). As previously explained, it could be suggested that the beach surface is regarded as relatively smooth due to the high VV backscatter observed. However, the forward scattering mechanism can be ruled out at some areas, due to the brightness of the radar image, suggesting a strong return signal, as opposed to the signal being scattered away (Alaska Satellite Facility, 2022).

The beach at Scratby Beach has cliffs present, and this site was chosen to contrast the influence of cliffs on the radar backscatter. It is thought that the presence of cliffs would result in a greater amount of diffuse-type double bounce scattering (Rosenqvist et al., 2018). However, upon comparison of the backscattering coefficients at Scratby Beach, compared to the other sandy beaches where cliffs were not present, these backscattering coefficients are not distinguishable. This suggests that the cliffs are not having a big influence on the radar return signal. This could be attributed to the fact that the cliffs may only affect a small area at the back of the beach, rather than all of the beach. This is significant as a mean backscattering coefficient across all the beach was taken, and so if the presence of cliffs only has an influence on the backscatter from a few pixels, this would have a limited effect on the overall mean average.

5.4 Sediment Size and NovaSAR S-band SAR

The backscattering coefficient values for NovaSAR data ranged from -11.43 dB to -2.12 dB. Saini et al., (2020) studied the backscattering coefficient of different land uses in India. The dB values found in this study were found to be most similar to the backscattering coefficient Saini et al., (2020) found to be indicative of sub-urban areas. This could be feasible, as sub-urban areas may consist of stones and sandy areas, which are found on beaches, as opposed to hard concrete. However, they used a HH polarisation, compared to the VV polarisation used in this study, so there can be expected to be some disparities when comparing the results in this study to those found in the study by Saini et al., (2020).

Results show that there is a moderate positive correlation, of 0.4871, between median sediment size and the mean backscattering coefficient when using the data from the S-band SAR satellite, NovaSAR-1 (Figure 21). NovaSAR has a wavelength of 75-150 mm (Herndon et al., [online], 2019), which is much bigger than the site with the largest sediment size used in this study, which measures 64.7 mm. Natale et al., (2011) states that the applications of S-band SAR are most likely to be similar to those of C-band SAR, hence why S-band SAR was chosen to be investigated in this study. However, the correlation between the variables using S-band SAR is weaker than the correlation observed using C-band SAR.

It is hypothesised that the NovaSAR S-band SAR is unlikely to be able to determine sediment size. This is due to the larger wavelength of S-band SAR, as mentioned above, and the fact that it is much bigger than the largest sediment in this study. Therefore, interactions between the S-band radar and the sediment will be expected to be a lot less. However, Wu et al., (2019) found a strong positive correlation between the backscattering coefficient and median sediment size, using ALOS-2's PLASAR-2 L-band sensor, which has a bigger wavelength than S-band SAR, of ~240 mm. The sediment grain size in their study ranges from 0.1 mm to approximately 120 mm (Wu et al., 2019), much smaller than the wavelength of L-band SAR. Therefore, the literature suggests that using a wavelength bigger than the spatial diameter of the sediment does not necessarily mean that there will not be a correlation between the variables.

However, different beaches are also a lot easier to distinguish in the NovaSAR data than in the Sentinel-1 data. As shown in Figure 21, the NovaSAR backscattering coefficients observed from Chesil Beach have a similar value, despite the graded change in sediment grain size. Additionally, Aldeburgh Beach has much higher dB values observed with the NovaSAR data than the dB values observed from the area at Chesil Beach with the same sediment size. This is in comparison to Sentinel-1 data, where, in general, dB values at Aldeburgh are similar in the VV polarisation. When the correlation is calculated for the NovaSAR dB values for Chesil Beach independently, the Pearson's correlation coefficient

is not statistically significant, showing no correlation between the sediment size and the backscattering coefficient using NovaSAR data. This suggests that there are other factors, potentially the shape of the beach or other characteristics, which are having an influence on the dB values at each beach, rather than the actual sediment grain size. However, further research will have to be undertaken into the exact factors, as this is beyond the scope of this study. From this, it is concluded that the use of C-band SAR is preferable to the use of S-band SAR for this application.

Advantageously, the fact that no correlation is observed for graded sediment using S-band SAR, but a strong correlation is found when using C-band SAR provides additional evidence that the variation in sediment grain size is influencing the backscatter from Sentinel-1. Especially as NovaSAR is sensitive to surface roughness (CSIRO, 2021) and no variations in NovaSAR backscatter are observed from Chesil Beach, despite a change in surface roughness along this beach as seen from the beach profiles (Figure 19). This suggests that although there is a change in surface roughness, the change may be too small from this beach to have a big effect on the backscatter.

There are no publications to date using the backscatter from NovaSAR or S-band SAR to determine sediment grain size, so therefore this research is entirely exploratory, with no literature to refer to.

5.5 Beach Elevation and Gradient

Results show that there is a strong positive correlation, of 0.7712, between the average beach gradient and sediment size. This agrees with the well-studied relationship that a steeper beach gradient is indicative of coarser beach sediment (Bascom, 1951; Bujan et al., 2019; McFall, 2019). However, from the plotted graph, there is only a moderate linear relationship between the two variables, with a R^2 value, of 0.5948. This shows that the data does not fit the linear regression model as well as hypothesised. This relatively poor fit can be explained by the disparities between the sediment size and the gradients of the beaches, with beaches that have a similar sediment size having varying gradients. For example, Aldeburgh Beach has sediments in the range of 30.3 – 39.3 mm, similar to sediment at the Visitors Centre at Chesil Beach, which has sediment in the range of 33.6 – 37.5 mm, yet the average beach gradient was less at Aldeburgh, with the median gradient across all sites at Aldeburgh is 0.1160, compared to 0.1616 at the Visitors Centre at Chesil. This suggests that although a higher beach gradient is indicative of coarser sediment size, the sediment size cannot be accurately predicted from the gradient of the beach.

Beach slope is one of the factors which can influence SAR backscatter (Stark et al., 2018). In the study by Stark et al., (2018), they assumed that the beach slope was constant between different areas, however, evidently this is not the case for the field sites in this study. Despite the variation in beach slope, when the backscatter intensity is plotted against sediment size (Figure 14), there is little variation in backscatter intensity for those areas of similar sediment size, irrespective of beach gradient. For instance, as discussed above, even though there is a difference in average beach gradient at Aldeburgh and Chesil Beach Visitor Centre (Figure 20), the backscatter intensity in both polarisations is similar, with Chesil Beach having only a slightly higher backscatter intensity than Aldeburgh Beach in both VV and VH polarisations. Site C7 and Site A4 both had the exact same median sediment size, of 37.4 mm, and had an average, across the two SAR images, VV intensity of 0.2001 and 0.1627 respectively, despite an elevation difference of almost 7 m at the highest point of the beach (Figure 18) and a gradient difference of 0.0456 (Figure 20). With elevation and average gradient differing,

but only a small difference in backscatter intensity, this suggests that the sediment size is having a greater influence on the backscatter intensity as opposed to the elevation and the beach slope. In addition, although sediment sizes at the sites were within mm of each other, Aldeburgh Beach has a slightly smaller overall median sediment size in general. It is also worth noting that Aldeburgh Beach has a lower gradient and maximum elevation than the areas at Chesil Beach with ~20 mm sediment size, yet has a greater backscatter intensity than these areas, therefore providing additional evidence that the greater backscatter intensity observed can be attributed to the sediment size on the beach.

5.6 Soil Moisture

Tide data shows that at Chesil and Aldeburgh Beach, the water table would have been too low to influence soil moisture at the time of the SAR data acquisition. Sediments were also measured from the dry area of the beach, i.e., not by the sea. Brakenhoff et al., (2019) states that if the beach elevation is greater than 0.5 m above the high tide level, then the water table will be too deep to influence the soil moisture. On the days in which SAR imagery were collected, the elevation of the beach exceeded the high-tide level for that day at both Chesil and Aldeburgh Beach. Additionally, by using ground-penetrating radar at Chesil Beach, Bennet et al., (2009) found that the water table is approximately 6 m below the highest elevation at Portland and Abbotsbury, which is greater than the 0.5 m threshold outlined by Brakenhoff et al., (2019). Therefore, it can be concluded that soil moisture is not affecting the radar data at Chesil Beach.

However, at the sandy beaches, the high tide (0.5 m) often exceeded most of the beach area in which backscatter was averaged over. This means that soil moisture could have had an impact on the SAR backscatter. However, all the SAR imagery taken over the sandy beaches were taken at a time of low or outgoing tide on the beach, where in lots of the beach would be above the tide level, meaning that soil moisture would not have had an as big impact.

5.7 Unknown Area

Each of the lines of best fit equations from Figures 14 and 15 were used to predict the sediment grain size by inserting the backscatter values from Sentinel-1 data from the unknown area into the line of best fit equations to determine whether the sediment grain size can be predicted from SAR backscatter.

Out of all the predictions, the line of best fit from the VH backscattering coefficient from Figure 15 had the closest prediction, of 36.1 mm, to the actual value measured from field samples, which was found to be 33.4 mm. This gives a disparity of 2.7 mm between the actual and predicted values, an error of only ~7.5 %.

It was expected that the value with the greatest R^2 value, and thus, had the best fit to the data would have the closest prediction. This was not the case, although the VV intensity line of best fit, with the highest R^2 value, resulted in the second closest prediction. Using the line of best fit which represents VV dB predicted the median sediment to be 44.4 mm, a value much bigger than the actual value, and further away from the actual value than the VH prediction, despite having a greater R^2 value than the line of best fit representing VH dB.

Considering that the line of best fit is not a perfect model, meaning that there will always be some error, this gives a good indication that it is possible to predict sediment size on

beaches from SAR backscatter. This is very promising, as there are approximately 6,000 shingle beaches in the UK (Southsea Coastal Scheme, 2018), meaning that there is a potential to survey sediment size on 6,000 beaches. This is of great importance, as beach surveying is very time consuming (Cabezas-Rabadán et al., 2021) and therefore, up-to-date records of beach grain size are rare.

If more data samples were available, machine learning models could be used to predict the sediment size on multiple beaches. This is beyond the scope of the study, as quantifying sediment grain size from backscatter is not one of the main objectives outlined in this study. Therefore, this is an addition and not the main part of the study.

5.8 Limitations

One limitation of this study was that only two Sentinel-1 SAR and only one NovaSAR images were analysed. This was due to time constraints of the project and complexity of the data processing and methodology. In addition, time constraints limited the amount of fieldwork that could be carried out. This meant that all fieldwork was carried out in one month, May 2022, and as beaches are dynamic environments, the median size would be expected to change. This meant the fieldwork carried out only captured the sediment size for a small time of the year. Furthermore, due to the limited time available for fieldwork, only 5 beaches were surveyed and only 1 unknown beach was used to predict median sediment grain size. Therefore, due to the time restraints, it was beyond the scope of this study to apply the research to use in real world applications, e.g., using SAR to analyse sediment transportation and changes in sediment grain size after storm and mass-erosion events.

Another limitation was the use of the Wolman's (1922) pebble count methodology. This methodology has been criticised in some studies as being biased and thought to overestimate grain size (Harvey et al., 2022; Strom et al., 2010). However, this method has been used successfully in other studies, such as that by Lees et al., (2022) and was determined the best method given equipment and time constraints.

5.9 Further Research

Suggestions for further study include the use of X-band radar for this application. X-band SAR is better at providing information about the top surface (Saini et al., 2020), which would be useful in this instance. C-band SAR has a stronger correlation between the backscattering coefficient and sediment size, compared to S-band SAR, and one of the suggestions put forward as to why this could be the case, is due to the smaller wavelength of C-band SAR. Therefore, X-band SAR, equipped with a smaller wavelength could be better at interacting with beach sediment, which are often smaller than the wavelength of C-band SAR.

Further research would also include collecting more data for a greater amount of field locations over the course of a longer time-period, e.g., a year. As more data was added to the models, the R^2 value increased, meaning that the model fit the data better. Adding more field sites will also allow an assessment over a range of different areas with different geomorphologies. Collecting data over a longer time period will allow for an assessment of how this research can be applied to real-world situations, such as an assessment of how sediment changes throughout the year and if radar can pick up this change, as this would be one of the main benefits of this research.

If more data was able to be collected, machine learning models could be implemented to make more accurate predictions on the median sediment grain size. This was unable to

be done in this study due to the limited amount of data collected, due to the time constraints of fieldwork.

Fieldwork taking surface roughness measurements or a metric to quantify this would need to be included in further research to compare surface roughness with both backscattering coefficient and sediment grain size. Some of the evidence in this study shows that the roughness has a big impact on the backscattering coefficient, so this will need to be assessed in further detail.

Furthermore, away from beaches, this research can be applied to study areas and landforms with changing sediment grain size, e.g., alluvial fans, to affirm whether it is the grain size that is influencing the radar backscatter, by further ruling out the other factors that are specific to beaches, which also have an influence. A study by Aquino et al., (2013) have used DEMs derived from SAR and LiDAR imagery to outline the location of alluvial fans, but there have been no studies to date which use SAR data to quantify the specific change in grain size in alluvial fans.

6. CONCLUSION

In conclusion, results from this study show that there is a strong positive correlation between sediment grain size on beaches and backscatter from C-band Sentinel-1 data, showing that as sediment grain size increases, as does the mean backscattering coefficient. This overall conclusion agrees with the hypothesis of this study and agrees with the limited existing literature which have studied this relationship previously and also found a strong positive correlation between the two variables (Wu et al., 2019; van der Wal et al., 2005).

The results indicate that the grain size of the beaches which consist of stones specifically are most positively correlated with C-band radar backscatter. When these values were plotted independently of the sandy beaches, there is a clear positive linear relationship between the two variables. There was, however, no correlation between the median sediment grain size of sand and the backscattering coefficient, showing that the grain size of the sand on sandy beaches cannot be determined by SAR.

It can be observed that the backscattering coefficient is greater in the VV polarisation compared to the VH polarisation. As co-polarisation is more indicative of smoother surfaces (Woodhouse, 2006), this suggests that overall, the beach surface is regarded as smooth, with less distinction between different beaches in this polarisation, regardless of the difference in elevation and roughness. However, the difference between VV and VH polarisations became less as the median sediment grain size increased. This could be because as sediment increases, so does surface roughness. This can be observed from the beach profiles plotted along with the fact that VH polarisation is more sensitive to surface roughness (Woodhouse, 2006).

A moderate positive correlation was found between sediment grain size on beaches and backscatter from S-band NovaSAR data. However, the backscattering coefficients varied between different beaches and did not show a clear, integrated linear relationship across all beaches like Sentinel-1 data did. Most notable, a change in the backscattering coefficient along Chesil Beach was not observed. There was no correlation between the two variables, despite the graded sediment size occurring along this beach. This shows that the variations in backscattering coefficient from the different beaches observed from the NovaSAR data is not caused as a result of the sediment grain size and is instead caused by other factors. However, due to the limited literature available, further research is required into the cause of the difference in the backscatter between the different beaches.

In general radar interacts with targets of the same or bigger spatial magnitude as its wavelength (Rosenqvist et al., 2018), so it was not expected that there would be a correlation between NovaSAR backscatter and sediment grain size. This is due to the bigger wavelength of S-band SAR, of 7.5-15 cm (Herndon [online], 2019), which is larger than the biggest median sediment grain size in the study. However, the fact that there was no correlation observed between the variables along Chesil Beach, yet a clear linear relationship was observed when using the Sentinel-1 C-band SAR, which has a lower wavelength of 3.8-7.5 cm (Herndon [online], 2019), similar to some of the median sediment grain size in this study, adds additional evidence that the backscattering coefficient is being influenced by the sediment with Sentinel-1 data.

Due to this observation, it is determined that the use of C-band SAR is more desirable than the use of S-band SAR for this application. Suggested further research includes the use of X-band SAR, which has the smallest SAR wavelength available.

Surface roughness was one of the main components highlighted that influences SAR backscatter (Deroin, 2020; Van der Wal et al., 2005). Although this potentially could have had an influence on the correlation observed, as beach surface roughness increased as sediment grain size increased, NovaSAR data is also sensitive to surface roughness (CSIRO, 2021), yet no variation in backscatter is observed from Chesil Beach. This suggests that the change in surface roughness is having minimal impact on the backscatter, potential because it is too minimal. This provides more evidence that the C-band SAR is sensitive to the sediment grain size. However, further research to quantify surface roughness, either through field data collection or through a metric, is needed to define this relationship, as this was beyond the scope of this study.

Soil moisture was able to be ruled out as one of the factors which influenced SAR backscatter on stony beaches, due to these beaches having elevations greater than the water table, which was defined, by Brakenhoff et al., (2019) as the tidal level +0.5 m.

Overall, this research has shown that there is a strong positive correlation between the median sediment grain size on beaches and the SAR backscattering coefficient for C-band Sentinel-1 SAR. It has also shown that there is a potential to accurately predict sediment grain size on beaches from radar backscatter intensity.

It is hoped that this research will provide a basis for the ability for quick surveying of sediment grain size on beaches independent of weather to help tackle pressing global issues such as coastal erosion, to monitor sediment transportation and changes in sediment size, and to evaluate the effects of storms on beach characteristics. This research also has the potential to provide a foundation for further research into using radar to assess the grain size of materials in other environments, such as river sediments and alluvial fans.

REFERENCES

Alaska Satellite Facility. (2022). *How do I interpret SAR images?* [Online]. NASA Earth Data. Available at: https://asf.alaska.edu/information/sar-information/how-do-i-read-sar-images/ [Accessed 7 August 2022].

Aquino, D.T., Ortiz, I., Timbas, N., Gacusan, R., Montalbo, K., Eco, R.C. and Lagmay, A., (2013, December). Alluvial Fan Delineation from SAR and LIDAR-Derived Digital Elevation Models in the Philippines. In *AGU Fall Meeting Abstracts*, *2013*, pp. NH33A-1631.

Bascom, W.N., (1951). The relationship between sand size and beach face slope. *Eos, Transactions American Geophysical Union*, 32(6), 866–874.

Bennett, M.R., Cassidy, N.J. and Pile, J., (2009). Internal structure of a barrier beach as revealed by ground penetrating radar (GPR): Chesil beach, UK. *Geomorphology*, *104*(3-4), pp.218-229.

Bio, A., Bastos, L., Granja, H.M., Pinho, J.L., Gonçalves, J.A., Henriques, R.F., Madeira, S., Magalhães, A. and Rodrigues, D., (2015). Methods for coastal monitoring and erosion risk assessment: two Portuguese case studies.

Bird, E.C., (1996). Lateral grading of beach sediments: a commentary. *Journal of Coastal Research*, pp.774-785.

Bird, R., Whittaker, P., Stern, B., Angli, N., Cohen, M. and Guida, R., (2013, September). NovaSAR-S: A low cost approach to SAR applications. In *Conference Proceedings of 2013 Asia-Pacific Conference on Synthetic Aperture Radar (APSAR)* (pp. 84-87). IEEE.

Born, G.H., Dunne, J.A. and Lame, D.B., (1979). Seasat mission overview. *Science*, *204*(4400), pp.1405-1406.

Brakenhoff, L.B., Smit, Y., Donker, J.J. and Ruessink, G., (2019). Tide-induced variability in beach surface moisture: observations and modelling. *Earth Surface Processes and Landforms*, *44*(1), pp.317-330.

Bujan, N., Cox, R. and Masselink, G., (2019). From fine sand to boulders: Examining the relationship between beach-face slope and sediment size. *Marine Geology*, *417*, p.106012.

Burns, J.J., (2019). *Using LiDAR derivatives to estimate sediment grain size on beaches in False Bay* (Doctoral dissertation, Stellenbosch: Stellenbosch University). Available: http://scholar.sun.ac.za/handle/10019.1/107062

Cabezas-Rabadán, C., Pardo-Pascual, J.E. and Palomar-Vázquez, J., (2021). Characterizing the Relationship between the Sediment Grain Size and the Shoreline Variability Defined from Sentinel-2 Derived Shorelines. *Remote Sensing*, *13*(14), p.2829.

Carr, A.P., (1969). Size grading along a pebble beach; chesil beach, England. *Journal of Sedimentary Research*, *39*(1), pp.297-311.

Chardon, V., Schmitt, L., Piégay, H. and Lague, D., (2020). Use of terrestrial photosieving and airborne topographic LiDAR to assess bed grain size in large rivers: a study on the Rhine River. *Earth Surface Processes and Landforms*, *45*(10), pp.2314-2330.

Copernicus Open Access Hub. (2022). *Copernicus Open Access Hub.* [Online]. Available at: https://scihub.copernicus.eu/ [Accessed 1 August 2022].

CSIRO. (2021). *NovaSAR-1 satellite.* [Online]. CSIRO Facilities Collections. Last Updated: 25 February 2021. Available at: https://www.csiro.au/en/about/facilities-collections/novasar-1 [Accessed 10 August 2022].

Davis, R.A. and FitzGerald, M. (2004). Beach and nearshore environment. In: Davis, R.A. and FitzGerald, M. (Ed). Beaches and Coasts. Oxford: Blackwell. pp.115-130.

Deroin, J.P., (2020). Potential of Sentinel 1 Satellites for Mapping Tidal Flats. Case Study of the Baie Des Veys (Normandy, France). In *IGARSS 2020-2020 IEEE International Geoscience and Remote Sensing Symposium* (pp. 5733-5736). IEEE.

Enomoto, K., Sakurada, K., Wang, W., Kawaguchi, N., Matsuoka, M. and Nakamura, R., (2018, July). Image translation between SAR and optical imagery with generative adversarial nets. In *IGARSS 2018-2018 IEEE International Geoscience and Remote Sensing Symposium* (pp. 1752-1755). IEEE.

ESA. (2022a). *Definitions.* [Online]. ESA User Guides - Sentinel-1 SAR. Available at: https://sentinels.copernicus.eu/web/sentinel/user-guides/sentinel-1-sar/definitions#:~:text=Backscat [Accessed 22 July 2022].

ESA. (2022b). *Mission ends for Copernicus Sentinel-1B satellite.* [Online]. ESA. Last Updated: 3 August 2022. Available at: https://www.esa.int/Applications/Observing_the_Earth/Copernicus/Sentinel-1/Mission_ends_for_Copernic [Accessed 12 August 2022].

Garestier, F., Bretel, P., Monfort, O., Levoy, F. and Poullain, E., (2014). Anisotropic surface detection over coastal environment using near-IR LiDAR Intensity maps. *IEEE Journal of Selected Topics in Applied Earth Observations and Remote Sensing, 8*(2), pp.727-739.

Geudtner, D., Torres, R., Snoeij, P., Davidson, M. and Rommen, B., (2014, July). Sentinel-1 system capabilities and applications. In *2014 IEEE Geoscience and Remote Sensing Symposium* (pp. 1457-1460). IEEE.

Harley, M.D., Masselink, G., Ruiz de Alegría-Arzaburu, A., Valiente, N.G. and Scott, T., (2022). Single extreme storm sequence can offset decades of shoreline retreat projected to result from sea-level rise. *Communications Earth & Environment*, *3*(1), pp.1-11.

Harvey, E.L., Hales, T.C., Hobley, D.E., Liu, J. and Fan, X., (2022). Measuring the grain-size distributions of mass movement deposits. *Earth Surface Processes and Landforms*.

Herndon, K., Meyer, F., Flores, A., Cherrington, E., and Kucera, L. (2019). *What is Synthetic Aperture Radar?* [Online]. NASA Earth Data. Available at: https://www.earthdata.nasa.gov/learn/backgrounders/what-is-sar [Accessed 19 July 2022].

IPR. (2022). *Roughness and Brightness of SAR Image.* [Online]. IPR: Quick Image Processing Research Guide. Last Updated: 5 February 2022. Available at: https://www.gofastresearch.com/2022/02/roughness-and-brightness-of-sar-image.html [Accessed 10 August 2022].

Kim, K.L., Kim, B.J., Lee, Y.K. and Ryu, J.H., (2019). Generation of a large-scale surface sediment classification map using unmanned aerial vehicle (UAV) data: A case study at the Hwang-do tidal flat, Korea. *Remote Sensing*, *11*(3), p.229.

Lees, D.C., Hein, C.J. and FitzGerald, D.M., (2022). Measuring Organization of Large Surficial Clasts in Heterogeneous Gravel Beach Sediments. *Journal of Marine Science and Engineering*, *10*(4), p.525.

Liew, S.C. (2001). *SAR Images.* [Online]. CRISP: Centre for Remote Imaging, Sensing and Processing. Available at: https://crisp.nus.edu.sg/~research/tutorial/sar_int.htm [Accessed 10 August 2022].

Living on the Edge. (2019). *Living on the edge*. [Online]. confused.com. Available at: https://www.confused.com/home-insurance/living-on-the-edge?awc=4445_1658493576_557af231f0fe98d811502 [Accessed 22 July 2022].

Long, B., Xharde, R., Boucher, M. and Forbes, D., (2006), July. Significance of LiDAR return signal intensities in coastal zone mapping applications. In *2006 IEEE International Symposium on Geoscience and Remote Sensing* (pp. 2424-2427). IEEE.

Lurton, X., Lamarche, G., Brown, C., Lucieer, V.L., RIce, G., Schimel, A. and Weber, T., (2015). Backscatter measurements by seafloor-mapping sonars: guidelines and recommendations. *A collective report by members of the GeoHab Backscatter Working Group*, (May), pp.1-200.

Masselink, G., Russell, P., Rennie, A., Brooks, S. and Spencer, T., (2020). Impacts of climate change on coastal geomorphology and coastal erosion relevant to the coastal and marine environment around the UK. *MCCIP Science Review, 2020*, pp.158-189.

McCave, I.N., (1978). Grain-size trends and transport along beaches: example from eastern England. *Marine Geology*, *28*(1-2), pp.M43-M51.

McFall, B.C., (2019). The relationship between beach grain size and intertidal beach face slope. *Journal of Coastal Research*, *35*(5), pp.1080-1086.

Natale, A., Guida, R., Bird, R., Whittaker, P., Cohen, M. and Hall, D., (2011, September). Demonstration and analysis of the applications of S-band SAR. In *2011 3rd International Asia-Pacific Conference on Synthetic Aperture Radar (APSAR)* (pp. 1-4). IEEE.

ONS. (2020). *Coastal towns in England and Wales: October 2020.* [Online]. Office for National Statistics. Last Updated: 6 October 2020. Available at: https://www.ons.gov.uk/businessindustryandtrade/tourismindustry/articles/coastaltowns inenglandandwales/2020-10-06#:~:text=Over%205.3%20million%20residents%20live,2020%20than%20non%2Dco astal%20towns. [Accessed 24 August 2022].

Potin, P., Rosich, B., Grimont, P., Miranda, N., Shurmer, I., O'Connell, A., Torres, R. and Krassenburg, M., (2016, June). Sentinel-1 mission status. In *Proceedings of EUSAR 2016: 11th European Conference on Synthetic Aperture Radar* (pp. 1-6). VDE.

Poulton, C.V., Lee, J., Hobbs, P., Jones, L. and Hall, M., (2006). Preliminary investigation into monitoring coastal erosion using terrestrial laser scanning: case study at Happisburgh, Norfolk. *Bulletin of the Geological Society of Norfolk*, pp.45-64.

Rosen, J. (2021). *Shifting Ground: Fleets of radar satellites are measuring movements on Earth like never before.* [Online]. Science. Last Updated: 25 February 2021. Available at: https://www.science.org/content/article/fleets-radar-satellites-are-measuring-movements-earth-never [Accessed 18 August 2022].

Rosenqvist, A., Perez, A. and Olfindo, N., (2018). A Layman's Interpretation Guide to L-band and C-band Synthetic Aperture Radar data. *Comittee on Earth Observation Satellites: Washington, DC, USA*.

Saini, O., Bhardwaj, A. and Chatterjee, R.S., (2020, March). Analysis of Back-Scattering Coefficient of NovaSAR-1 S-Band SAR. In *Proceedings of the National Seminar on Recent Advances in Geospatial Technology and Application, Dehradun, India* (pp. 117-122).

Sano, E.E., Huete, A.R. and Moran, M.S., (1999). Estimation of surface roughness in a semiarid region from C-band ERS-1 synthetic aperture radar data. *Revista brasileira de ciência do solo, 23*, pp.903-908.

SEDAS. (2022). *SEDAS Portal.* [Online]. Available at: http://geobrowsertest.satapps.org/#mapviewer:undefined [Accessed 1 August 2022].

SentinelHub. (2022). *SentinelHub Playground*. [Online]. Available at: https://apps.sentinel-hub.com/sentinel-playground/?source=S2L2A&lat=52.17384396775459&lng=1.60497665 [Accessed 15 August 2022].

Southsea Coastal Scheme. (2018). *Southsea's Shingle*. [Online]. Southsea Coastal Scheme. Available at: https://southseacoastalscheme.org.uk/wp-content/uploads/2018/04/8.-Shingle-Factsheet.pdf [Accessed 10 August 2022].

Stark, N., Sheppard, J., Graber, H.C., McNinch, J.E. and Wadman, H.M., (2018), June. Geotechnical Characterization of Beach Sediments using SAR: Ideas, Challenges and Preliminary Data. In *EUSAR 2018; 12th European Conference on Synthetic Aperture Radar* (pp. 1-4). VDE.

Strom, K.B., Kuhns, R.D. and Lucas, H.J., (2010). Comparison of automated image-based grain sizing to standard pebble-count methods. *Journal of Hydraulic Engineering*, *136*(8), pp.461-473.

Tide Times. (2022). *Tide Times.* [Online]. Available at: https://www.tidetimes.org.uk/ [Accessed 24 August 2022].

Time and Date. (2022). *Time and Date.* [Online]. Available at: https://www.timeanddate.com/ [Accessed 24 August 2022].

Uncles, R.J., Clark, J.R., Bedington, M. and Torres, R., (2020). On sediment dispersal in the Whitsand Bay Marine Conservation Zone: neighbour to a closed dredge-spoil disposal site. In *Marine protected areas* (pp. 599-629). Elsevier.

UN SPIDER. (2022). *Step-by-Step: Mudslides and Associated Flood Detection Using Sentinel-1 Data.* [Online]. United Nations Office for Outer Space Affairs UN-SPIDER Knowledge Portal. Available at: https://www.un-spider.org/advisory-support/recommended-practices/mudslides-flood-sentinel-1/step-by- [Accessed 12 August 2022].

Van Der Wal, D. and Herman, P.M., (2007). Regression-based synergy of optical, shortwave infrared and microwave remote sensing for monitoring the grain-size of intertidal sediments. *Remote Sensing of Environment*, *111*(1), pp.89-106.

Van Der Wal, D., Herman, P.M. and Wielemaker-van Den Dool, A., (2005). Characterisation of surface roughness and sediment texture of intertidal flats using ERS SAR imagery. *Remote sensing of environment*, *98*(1), pp.96-109.

Vitousek, S., Barnard, P.L. and Limber, P., (2017). Can beaches survive climate change? *Journal of Geophysical Research: Earth Surface*, *122*(4), pp.1060-1067.

Wentworth, C.K., (1922). A scale of grade and class terms for clastic sediments. *The journal of geology, 30*(5), pp.377-392.

Whittaker, P., Doody, S., Cohen, M., Schwarz, B., Burbidge, G. and Bird, R., (2021, March). NovaSAR-1–Early mission achievements. In *EUSAR 2021; 13th European Conference on Synthetic Aperture Radar* (pp. 1-4). VDE.

Wiley, C.A., (1985). Synthetic aperture radars. *IEEE Transactions on Aerospace and Electronic Systems*, (3), pp.440-443.

Williams, A.T., Rangel-Buitrago, N., Pranzini, E. and Anfuso, G., (2018). The management of coastal erosion. *Ocean & coastal management*, *156*, pp.4-20.

Wolman, M.G., (1954). A method of sampling coarse river-bed material. *EOS, Transactions American Geophysical Union, 35*(6), pp.951-956.

Woodhouse, I.H. (2006). Polarimetry. In: Woodhouse, I.H. (Ed). Introduction to Microwave Remote Sensing. Boca Raton, FL : Taylor & Francis. pp.65-92.

Wu, L., Tajima, Y., Yamanaka, Y., Shimozono, T. and Sato, S., (2019). Study on characteristics of SAR imagery around the coast for shoreline detection. *Coastal Engineering Journal*, *61*(2), pp.152-170.

Yates, M.G., Jones, A.R., McGrorty, S. and Goss-Custard, J.D., (1993). The use of satellite imagery to determine the distribution of intertidal surface sediments of the Wash, England. *Estuarine, Coastal and Shelf Science*, *36*(4), pp.333-344.

Zikra, M. and Suntoyo, H.W., (2017). Coastal Sediment Cells for the North Coast of East Java, Indonesia. *International Journal of Civil Engineering and Technology*, *8*(8), pp.1247-1255.

APPENDIX

Millimeters (mm)		Micrometers (μm)	Phi (φ)	Wentworth size class	
	4096		-12.0	Boulder	Gravel
	256		-8.0	Cobble	
	64		-6.0	Pebble	
	4		-2.0	Granule	
	2.00		-1.0		
	1.00		0.0	Very coarse sand	Sand
1/2	0.50	500	1.0	Coarse sand	
1/4	0.25	250	2.0	Medium sand	
1/8	0.125	125	3.0	Fine sand	
1/16	0.0625	63	4.0	Very fine sand	
1/32	0.031	31	5.0	Coarse silt	Silt
1/64	0.0156	15.6	6.0	Medium silt	
1/128	0.0078	7.8	7.0	Fine silt	
1/256	0.0039	3.9	8.0	Very fine silt	
	0.00006	0.06	14.0	Clay	Mud

Appendix A: Wentworth Grain Size Chart. Source: Wentworth (1922).

Task / W/B	Completion	04-Apr	11-Apr	18-Apr	25-Apr	02-May	09-May	16-May	23-May	30-May	06-Jun	13-Jun	20-Jun	27-Jun	04-Jul	11-Jul	18-Jul	25-Jul	01-Aug	08-Aug	15-Aug	22-Aug	29-Aug	05-Sep
Background Reading	100%	█	█	█	█	█	█																	
Draft Literature Review (Poster)	100%	█	█																					
Project Proposal	100%		█	█																				
Fieldwork Preperation	100%					█	█																	
Fieldwork: Scratby & Winterton	100%						█	█																
Fieldwork: Aldeburg	100%						█	█																
Fieldwork: Chesil	100%								█															
Lab Work	100%								█	█	█	█												
SAR Data Processing	100%							█	█	█	█	█							█					
Elevation and Gradient Analysis	100%							█	█	█	█	█												
SAR Data Analysis	100%							█	█	█	█	█				█								
Introduction	100%									█	█													
Literature Review	100%									█	█	█	█											
Methodology	100%									█	█	█	█	█										
Results	100%														█	█	█	█						
Discussion	100%																		█	█	█			
Conclusion	100%																			█	█			
Bibliography, Figures and Tables	100%									█	█	█	█	█	█	█	█	█	█	█				
Final Edits	100%																						█	
Submission	100%																						█	
Poster for CDT Annual Assembly	0%																						█	
Presentation for Annual Assembly	0%																						█	
Present at Annual Assembly	0%																							█

Appendix B: Project Management Gaant Chart.

1) Provide the title and briefly describe the aim and objectives of your MRes project.

Title: An Investigation into the Relationship Between Synthetic Aperture Radar (SAR) Data and Beach Sediment Grain Size

Aim: The aim of this study is to investigate the relationship between SAR backscatter and the sediment grain size on beaches.

Objectives:
1. To determine sediment grain size distribution on a range of beaches by constructing and carrying out a fieldwork methodology to collect ground-truth data for beach composition.
2. Evaluate if there is a correlation between backscatter from SAR imagery and sediment size.
3. Evaluate whether sediment size can be determined between the profile of a beach, specifically looking at the beach elevation and gradient.

2) What data will be produced? (Data types, format, standards, scale and method)

Primary data needed for the project will be obtained via fieldwork (collection of physical samples), which took place at 5 study sites across England, from 09/05/22 to 27/05/22.

The data which will be produced from the fieldwork will be:
- Sediment size – length, width, and depth. Measured using calipers (in field) or laser particle scanner (in lab) in mm. Recorded in an Excel file.
- Beach Elevation – using a GNSS receiver to receive elevation details of the area. Web-based online post-processing will be required. GNSS data will be in a RINEX file format.

Data will be recorded in paper format whilst in the field and transferred to a digital format as soon as possible (Excel file).

Secondary data used in the project will be primarily open source (except for NovaSAR data):
- SAR Data
  - Sentinel-1 – Resolution 10-18 m – Available for download from the Copernicus Open Access Hub https://scihub.copernicus.eu/dhus/ - data must be as recent as possible to fieldwork dates and/or fieldwork collection conditions – Open and Free from ESA and the European Commission. XML file format. (Storage: ~1.7 MB per image)
  - NovaSAR – Resolution 6m – Sourced from the UK Hydrographic Office (UKHO) – collection date: May, June 2022. Storage: ~1.5 MB per image.

To calculate the backscatter from the SAR data, the data will need to be processed in ESA's SNAP, a free open-source software from ESA. Pre-processing involved applying orbit files, speckle filtering, thermal noise removal, and ellipsoid/ terrain corrections, which are done by using the tools in the software.

After processing, the data will be exported to GeoTIFFs for analysis in QGIS. Storage: ~109 MB per image.

3) What metadata standards will you use? (Metadata content and format)

A 'metadata' folder will be created, consisting of .txt files for each dataset. Within these .txt files, details, including the units, geographical coordinates of fieldwork collection points and any other relevant information for the dataset will be included. The GNSS receiver will produce metadata, detailing location, accuracy, and satellite connection, which in turn will be uploaded in a file to the metadata folder.

As per EPSRC expectations, the metadata must be published on the internet within 12 months, ensuring that it has a digital object identifier (DOI), which is made available through DataCite. The metadata standards that will be used is the ISO 19115: Geographic information – Metadata Standard, which is an international schema for describing geospatial data.

4) How will your data be structured and stored? (Project storage)

Data will be stored on OneDrive. The University of Nottingham gives all its students access to 5TB of OneDrive storage, which will be more than enough for this project. If more storage is required, then Newcastle University also provides a further 5TB of OneDrive storage, which can also be made use of (using the respective email accounts I have for each university). The data will also be saved onto the hard drive of the laptop in which I have sole use over. Ensuring a strong password, which is changed regularly, on both OneDrive accounts and on my personal laptop is necessary to prevent hacking.

The raw data will be stored in a corresponding 'data' folder, for example, 'SAR_data'. Once processed, the images will be stored in a separate folder, for example, 'SAR_processed'.

Using the guide for storage for each data type above, the total storage required will be as follows: 4x Sentinel-1 images per study side (6.8 MB * 4 study sites = 27.2 MB), 8x NovaSAR (13.6 MB * 4 = 54.4 MB), 1x LiDAR data shapefile per study area (2.2 MB * 4 = 8.8 MB), 3x Sentinel-2 images per study site (2.01 MB * 4 = 8.04 MB).

Therefore, total storage of raw data = ~98 MB. This is therefore acceptable to store on 1 OneDrive folder.

5) How will the data be shared during and after the project? (Access, data sharing and reuse)

There is no sensitive data being used, with most data being open and freely available or collected by the researcher. Open-source software is being used for analysis to ensure reproducibility. During the research project, data and subsequent analysis will be shared with my supervisors as required. As outlined below, after the project, the data that has been used in the project will be uploaded to the Nottingham Research Data Management Repository and be held there for a minimum of 10 years.

6) Outline the approach to data selection and long-term preservation?

Data which are used in the final dissertation, along with the corresponding metadata will be placed in a zipped folder and deposited to the Nottingham data repository and made available in data archives for a minimum of 10 years. This service is free for data up to 50 GB. Once the data has been uploaded to the repository, the responsibility of maintaining the data will be down to the University of Nottingham IT Department and access to this data will be in line with the University policies.

7) Who has responsibility for implementing the DMP and are resources required?

The main researcher (Sophie Mann) will be responsible for the implementation of the DMP and for data validation. This DMP should be a dynamic document, and therefore, will be subject to changes as the project progresses. Each version of the DMP should be saved accordingly. The University of Nottingham IT Department will be responsible for maintaining the data once it has been uploaded to the repository.

Resources – I already have access to all software required.

- ESA SNAP – open-source software, which will be used to analyse SAR data.
- QGIS – open-source software, used to analyse LiDAR data and optical imagery.

Further training may be required, this will be sought from my supervisory team, the IT department, and my peers.

Appendix C: Data Management Plan.